RL-TR-93-56
Final Technical Report
May 1993

SYSTEM ARCHITECTURE OF OPTICALLY CONTROLLED PHASED ARRAY RADAR

University of California, Berkeley

K.Y. Lau

APPROVED FOR PUBLIC RELEASE; DISTRIBUTION UNLIMITED.

Rome Laboratory
Air Force Materiel Command
Griffiss Air Force Base, New York

This report has been reviewed by the Rome Laboratory Public Affairs Office (PA) and is releasable to the National Technical Information Service (NTIS). At NTIS it will be releasable to the general public, including foreign nations. RL-TR-93-56 has been reviewed and is approved for publication.

APPROVED:

DAVID A. CORDIERO
Project Engineer

FOR THE COMMANDER:

JOHN A. GRANIERO
Chief Scientist
Command, Control and Communications Directorate

If your address has changed or if you wish to be removed from the Rome Laboratory mailing list, or if the addressee is no longer employed by your organization, please notify RL (C3DB) Griffiss AFB NY 13441. This will assist us in maintaining a current mailing list.

Do not return copies of this report unless contractual obligations or notices on a specific document require that it be returned.

REPORT DOCUMENTATION PAGE

Form Approved
OMB No. 0704-0188

1. AGENCY USE ONLY (Leave Blank)	2. REPORT DATE	3. REPORT TYPE AND DATES COVERED
	MAY 1993	Final Aug 91 - Aug 92

4. TITLE AND SUBTITLE
SYSTEM ARCHITECTURE OF OPTICALLY CONTROLLED PHASED ARRAY RADAR

5. FUNDING NUMBERS
C - F30602-91-C-0057
PE - 63726F
PR - 2863
TA - 92
WU - PS

6. AUTHOR(S)
K.Y. LAU

7. PERFORMING ORGANIZATION NAME(S) AND ADDRESS(ES)
University of California, Berkeley
Department of Elect. and Computer Engineering
Berkeley CA 94720

8. PERFORMING ORGANIZATION REPORT NUMBER

9. SPONSORING/MONITORING AGENCY NAME(S) AND ADDRESS(ES)
Rome Laboratory (C3DB)
525 Brooks Road
Griffiss AFB NY 13441-4505

10. SPONSORING/MONITORING AGENCY REPORT NUMBER
RL-TR-93-56

11. SUPPLEMENTARY NOTES
Rome Laboratory Project Engineer: David A. Cordeiro/C3DB/(315)330-7120

12a. DISTRIBUTION/AVAILABILITY STATEMENT
Approved for public release; distribution unlimited.

12b. DISTRIBUTION CODE

13. ABSTRACT (Maximum 200 words)

The purpose of this effort is a study and analysis to explore architectural issues in Optically Controlled Phased Array Radar Systems, based upon progress in high speed, high efficiency, and low noise electro-optic devices and optical interconnections techniques. The aim is providing real time delay control signals for scanning of the radar beam over wide ranges of frequencies, and to simplify the hardware and power consumption at the antenna site.

14. SUBJECT TERMS
Phased array radar, electro-optical devices

15. NUMBER OF PAGES 52

16. PRICE CODE

17. SECURITY CLASSIFICATION OF REPORT	18. SECURITY CLASSIFICATION OF THIS PAGE	19. SECURITY CLASSIFICATION OF ABSTRACT	20. LIMITATION OF ABSTRACT
UNCLASSIFIED	UNCLASSIFIED	UNCLASSIFIED	U/L

CONTENT

1. Introduction
2. Noise Figure of microwave fiber-optic links
   - 2.1 Relative Intensity Noise
     - 2.1.1 Intrinsic laser noise and noise translation
     - 2.1.2 A comparison of Fabry-Perot and DFB lasers
   - 2.2 Modulation efficiency
     - 2.2.1 Gain lever
     - 2.2.2 Impedance matching
3. Narrow band millimeter wave modulation by photomixing and feedforward compensation
   - 3.1 Theory of operation
   - 3.2 Experimental demonstration
   - 3.3 Optimization of parameters
4. Conclusion

1. Introduction

The prime objective of this contract is to examine the optimum system configuration to best ultilize recently advanced optoelectronic components and technology in phased array systems. While the conceptual advantages of applying optics in phased array radar are numerous, its feasibility depends critically on the available optoelectronic technologies. The first and foremost problem one encounters is the relatively high throughput loss and a high noise figure of fiber-optic microwave links. The Noise Figure (N.F.), in particular, is a universal means of measuring the fidelity of any microwave component and represents an unrecoverable degradation in the signal quality upon passage through the device. The poor throughput arises from the unavoidable inefficiencies in optoelectronic devices and in optical coupling between components. These problems can be tackled by either raising the modulation efficiency of the transmitter, or by lowering the relative intensity noise of the laser, or both. We shall address both of these issues.

While past efforts have concentrated almost exclusively on microwave fiber-optic systems well within the modulation bandwidth of laser diodes or external modulators, which at present is limited to around 20-30GHz, one can look ahead into systems that operates in the millimeter wave regime where no transmitters are now available. To this end, we have developed a new concept of transmitting narrowband millimeter wave signals, **at any arbitrary center frequency over a bandwidth of a few gigahertz**, using a feedforward concept in conjection with the mixing product of two laser diodes. This approach, as with all other approaches, has its limitations (mainly in terms of noise characteristics). We have completed a quantitative study of the S/N ratio achievable using this approach, and conclude that the system perfomance of this approach, at millimeter wave frequency, can be comparable to that of a typical high perfomance link at the lower GHz range using directly modulated lasers. We have demonstrated this technique at 8GHz and is currently pursuing a demonstrateion at 45GHz. This work is still, to this date even though the current contract has ended, being continued with temporary resouces and is expected to be supported by a new contract from Rome Laboratories.

2. Noise Figure of microwave fiber-optic links

As mentioned in the Introduction section, the first and foremost problem one encounters in high performance microwave fiber-optic links is the relatively high throughput loss and a high noise figure of fiber-optic microwave links. The Noise Figure (N.F.) will depend on both the transmitter noise and receiver noise, as well as the modulation efficiency of the transmitter. In general, the receiver is thermal noise limited, although for certain high-impedance front-end design this may not be the case. In any event, the noise from the transmitter is a most critical component in determining the overall noise figure of the link. We begin our discussion by considering the intrinsic relative intensity noise of the laser, and their interaction with optical components and applied modulation signal. Then we shall consider how to increase the modulation efficiency of the laser transmitter in order to lower up the overall noise figure of the system.

2.1 Relative Intensity Noise (RIN)

It is fairly straightforward, at least conceptually, to consider how a lower RIN can be accomplished. In general, RIN decreases with increasing power, until the shot noise limit is reached. Even so, the shot noise can still be lowered by a further increase of the optical power. A high power optical source is thus desirable, not specifically for power per se, but for its lower noise. Diode-pumped YAG lasers that lases in the 100mW range seems suitable for this purpose. However, these devices need to be externally modulated, with a relatively low modulation efficiency, so that the net N.F. is quite disappointing, despite the low RIN. On the other hand, the highest modulation efficiency can be obtained using gain-levered quantum-well lasers. One factor that always faces devices with high modulation efficiency is a reduced dynamic range. This is unavoidable unless one simultaneously boosts the maximum output power of the device.

To the extent that we are transmitting signals at microwave frequencies, it might be tempting to make the statement that only high frequency intensity noise in lasers are important for these applications. Low frequency noise observed in some laser diodes are therefore irrelevant to these systems. This is an erroneous assumption since, as we shall discuss below, that when an high frequency

applied modulation is present, low frequency noise can be "translated" to the vicinity of the high frequency carrier through intrinsic nonlinear effects in the laser diode, thus making these low frequency noises highly relevant for microwave systems. We shall discuss some of these effects below.

2.1.1 Intrinsic intensity noise and noise translation

The dynamic range of a microwave fiber-optic system is determined at the high end by intermodulation distortions discussed above, and at the low end by laser intensity noise. Many microwave systems have quite stringent dynamic range requirements that far exceed those of digital transmission. Laser noise usually dominates over receiver noise in high frequency systems because the transmission distance is limited mainly by fiber bandwidth instead of attenuation and as a result the optical power at the receiver is usually quite high. Laser noise is commonly quantified by the Relative Intensity Noise (RIN), which is the rms value of the intensity fluctuation normalized by the average intensity [1]. The overall intrinsic laser intensity noise behavior has been quite well characterized, with the noise spectral density peaking at the relaxation oscillation frequency, and the overall noise level dropping as the optical power is increased [2-4]. This general behavior can be explained quite satisfactorily by a model using the laser field equations with Langevin source terms. Figure 1 shows a typical measured RIN results of a 1.3μm DFB laser.

For multimode lasers, there exists low frequency intensity noise - mode partition noise, which is associated with mode competition in a multimode laser. This effect has been analysed in detail, and the general characteristics are shown in Fig. 2. In short, gain saturation tends to stabilize the total power fluctuation in the laser output, while there is little active mechanism to stabilize the distribution of energy between the modes in a multimode laser. The result is a large power fluctuation in each mode taken alone in a multimode laser. The power fluctuation spectrum of an isolated mode in a multimode laser, as shown in Fig. 2, has a much enhanced low frequency part, with enhancement factors as large as 40dB. As long as all the modes are launched with equal efficiency into an optical fiber system, the negative correlation of fluctuations between the modes cancels out one another and the resultant noise spectrum is not too differenct from that of a single mode laser emitting at

the same total power. Even a slight frequency discrimation in the transmission characteristics of the fiber system (either in group velocity or amplitude) upsets the delicate balance and produces enhanced noise at low frequencies (<1GHz).

This section summarizes the derivation of mode partition noise. The approach is a very standard one using multimode rate equations[5], and we simplify the results using a two mode approximation with one dominant similar to that in [6]. Let S_i be the photon density in the ith longitudinal mode. The multimode rate equations are[5]:

$$\frac{dN}{dt} = \frac{J}{ed} - \frac{N}{\tau_e} - v\sum_i g_i(N)S_i + F_N(t) \tag{1a}$$

$$\frac{dS_i}{dt} = v\Gamma g_i(N)S_i - \frac{S_i}{\tau_p} + R_{sp} + F_{Si}(t) \tag{1b}$$

where N is the carrier density, Γ is the optical confinement factor, J is the pump current density, d the thickness of the active region, τ_e is the recombination lifetime (radiative and non-radiative) of the carriers, τ_p is the photon lifetime, $g_i(N)$ is the optical gain of the ith mode as a function of the carrier density, expressed in cm^{-1}, v is the group velocity, R_{sp} is the spontaneous emission rate into each mode, and e the electronic charge. $F_N(t)$ and $F_{Si}(t)$ are Langevin noise sources driving the electrons and the modes; their correlation characteristics have been derived in detail[34,35,36]. The form of optical gain is assumed to be

$$g_i(N) = g'_{i0}(N - N_0)(1 - v\epsilon S_i) \tag{2}$$

where ϵ is the gain compression parameter, N_0 is the transparency electron density, and $g'_{(i0)}$ assumes a parabolic gain profile near the gain peak. Note that we have neglected the cross-compression terms between different longitudinal modes. Its effects has been studied previously[6], and is shown to produce a low frequency "mode-hopping noise" in situations where two or more longitudinal modes have almost equal power. The noise spectra are obtained by a small signal solution of Eq. (1), using the proper Langevin correlation characteristics. In the case of a nearly single mode laser ($S_1 \gg S_2$), one can obtain the noise spectra in closed (albeit approximate) form in an approach similar to that used in [6]:

$$s_1(\omega) = F_{s1}(\omega)A(\omega) - F_{s2}(\omega)B(\omega)) \tag{3a}$$

$$s_2(\omega) = F_{s2}(\omega)B(\omega)) \tag{3b}$$

where $s_1(\omega)$, $s_2(\omega)$ are Fourier transforms of the small signal modal fluctuations, $A(\omega)$ and $B(\omega)$ are given by

$$A(\omega) = \frac{i\omega + 1/\tau_R}{(i\omega)^2 + i\omega\gamma_1 + \omega_r^2} \tag{4a}$$

$$B(\omega) = \frac{i\omega + 1/\tau_R}{(i\omega)^2 + i\omega\gamma_2 + \delta\omega_r^2} \tag{4b}$$

where expressions for the corner frequencies ω_r, $\delta\omega_r$, the damping constants γ_1, γ_2 and the effective lifetime τ_R are

$$\gamma_{1,2} = \frac{R_{sp}}{S_{1,2}} + \frac{1}{\tau_R} + v\epsilon S_{1,2} \tag{4c}$$

$$\omega_r^2 \sim g_1' S_1/\tau_p \tag{4d}$$

$$\delta\omega_r^2 = \left[\frac{R_{sp}}{S_2} + v\epsilon S_2\right]\frac{1}{\tau_R} \tag{4e}$$

τ_R is the effective carrier lifetime (stimulated and spontaneous), $F_{s1}(\omega)$, $F_{s2}(\omega)$ are Fourier transforms of the Langevin noises driving the respective modes, with the following correlation relations[7]:

$$< F_{si}(\omega) F_{sj}^*(\omega) > = 2R_{sp} S_i \delta_{ij} \tag{5}$$

It has been assumed, as is customarily the case, that the Langevin force driving the electron reservoir ($F_N(t)$) is negligible.

The small signal fluctuation of the total power after propagating through a dispersive fiber is

$$s(\omega) = s_1(\omega) + k s_2(\omega) e^{i\omega dL} \tag{6}$$

where d, k and L are the differential delay between the two modes per unit length, relative coupling coefficient of the two modes into the fiber, and fiber length, respectively. The RIN is given by

$$\mathrm{RIN} \times (S_1 + S_2)^2 = < s(\omega) s^*(\omega) > \tag{7}$$

which can be evaluated using the correlation relation (6). The result is given by

$$\mathrm{RIN} \times S^2 = 2R_{sp}(S_1 |A(\omega)|^2 + S_2 |(1 - ke^{i\omega dL}) B(\omega)|^2) \tag{8}$$

where $S = S_1 + S_2$ is the total optical power.

As mentioned in the beginning of this section, when an high frequency applied modulation is present, low frequency noise can be "translated" to the vicinity of the high frequency carrier through intrinsic nonlinear effects in the laser diode. To evaluate this effect we assume that there are a few dominant lasing modes of roughly equal amplitudes and very nearly equal modal gain. We then use the perturbative approach developed for calculating intermodulation products[8] to calculate the beat noise. Let S_i represents the photon number in the *ith* mode and N be the electron density. The variables are then splitted into the following parts:

$$S_i = S_{0i} + s_{1i}e^{i\omega_0 t} + s_{2i}(\Omega) + s_{3i}(\omega = \omega_0 + \Omega) \tag{9a}$$

$$N = N_0 + n_1 e^{i\omega_0 t} + n_2(\Omega) + n_3(\omega = \omega_0 + \Omega) \tag{9b}$$

where the variables with subscripts 0,1,2 and 3 denotes respectively the steady state, modulation signal, low frequency fluctuation part, and the beat noise. Ω denotes the low frequency noise, and ω_0 is the signal frequency. The three components are shown schematically in Fig. 3. Assuming $s_{1i} >> s_{2i} >> s_{3i}$, $s_{1i}(n_1)$ can be determined independently using the small signal rate equations with a current modulation signal. The beat noise $s_{3i}(\omega)$ is then found by writing the small signal rate equations with drive terms derived from the products $n_1 s_{2i}$ $(s_{1i} n_2)$:

$$i\omega n_3 = -(\sum_i g_i(N_0 s_{3i} + S_{0i} n_3) + n_3 + D(\omega) \tag{10a}$$

$$i\omega s_{3i} = \gamma(g_i N_0 s_{3i} + g_i S_0 n_3 - s_{3i} + \beta n_3 + G(\omega)) \tag{10b}$$

where γ is the ratio of carrier spontaneous to photon lifetime, ß is the spontaneous emission factor, and g_i is the modal gain. The drive terms are given by

$$G(\omega) = \frac{g_i}{2}(n_2(\Omega)s_{1i}(\omega_0) + s_{2i}(\Omega)n_1(\omega_0) \tag{11a}$$

$$D(\omega) = \sum_i G(\omega) \tag{11b}$$

At this point two approximations are made: that the low frequency fluctuation in photon number in each mode is much greater than the fluctuation in electron number due to the gain saturation stabilization effect, so that only the second term in Eq. (11a) is retained, and that the modal gain in the dominant modes differs from each other by only parts in 10^4 and are thus all taken to be

equal in this calculation. The result for the beat noise s_3 (normalized to the modulation signal s_1) is given in the following:

$$\frac{s_3(\omega = \omega_0 + \Omega)}{s_1(\omega_0)} = \frac{1}{2}\frac{\sum_i s_{2i}(\Omega)}{S_0 + \beta}\left\{\frac{g(\omega)(S_0 + \beta + h(\omega))}{f(\omega)}\right\} \tag{12a}$$

where

$$s_3(\omega) = \sum_i s_{3i} \tag{12b}$$

$$g(\omega) = i\omega + \gamma(1 - N_0) \tag{12c}$$

$$h(\omega) = i\omega + 1 + \tau_0 \tag{12d}$$

$$f(\omega) = h(\omega)g(\omega) + \gamma N_0(S_0 + \beta) \tag{12e}$$

The LHS of Eq. (12a) represents the S/N ratio. The first factor on the RHS of Eq. (12a) is just the RIN value of the total low frequency intensity noise. Fig. 4 plots the factor contained in {} in Eq. (12a), which represents the translation factor from the low frequency noise to high frequencies due to the presence of a modulation signal. At frequencies approaching the relaxation oscillation frequency, there is almost a one-to-one translation of the low frequency RIN to the maximum achievable high frequency S/N. The measured data points shows a reasonable match to the theoretical plot of Fig. 4.

2.1.2. S/N ratio of fiber links consisting of Fabry-Perot and distributed feedback lasers

This section is concerned with a quantitative evaluation of the various sources of signal-induced noise in a high frequency analog, single mode fiber-optic link using directly modulated multimode (Fabry-Perot) and single-frequency (DFB) lasers. The signal-to-noise ratio in a typical fiber-optic link is commonly evaluated by treating the various sources of noises, such as relative intensity noise (RIN), mode partition noise, shot and thermal noises, etc., as additive quantities independent of the modulation signal. However, there are sources of noise which become prominent only in the presence of a modulation signal. This paper presents experimental and theoretical studies on this type of noise which arises from mode-partitioning in Fabry-Perot lasers, and interferometric phase-to-intensity

noise conversion in DFB lasers, the former incited by fiber dispersion and the latter by fiber reflections such as Rayleigh scattering. Both of these effects, which are well known, increase with fiber length, and so does the signal-induced noise instigated by these effects.

Historically, the development of high speed semiconductor lasers for microwave/analog applications took place with conventional Fabry-Perot (FP) lasers due to their simplicity in construction and analysis which lend themselves to convenient demonstrations of ideas related to speed alone. To this date, the highest bandwidth semiconductor laser has been demonstrated in Fabry-Perot lasers[9,10], although single-frequency lasers also show exceptional performances[11]. The multimode lasing spectrum of FP lasers will be an issue in any wideband systems due to fiber dispersion, even for wavelengths near (but not exactly at) the dispersion minimum. This problem may not be significant for many microwave applications since most of these systems operate in a relatively narrow band of subgigahertz, albeit centered at a high frequency of multi-gigahertz. A more serious concern is the manifestation of mode-partition noise due to fiber dispersion, a subject studied in considerable detail[5]. This type of noise usually does not extend to beyond a few hundred megahertz, and is not considered harmful to high frequency microwave systems, hence they need not be specified in such applications. A similar type of low-frequency noise, the "mode-hopping" noise[5,12,13], which can manifest itself in the laser diode output alone without the aid of fiber dispersion, was similarly considered not significant for microwave applications. However, it has been shown that in a directly modulated laser diode, the low frequency noise can be translated to the neighborhood of the modulation carrier[14]. This is a source of signal-induced noise for Fabry-Perot lasers that can become quite serious at high frequencies and longer fiber links. We shall quantify these parameters later. It is therefore a mistake to not consider low frequency noise in lasers for high frequency applications. Furthermore, it will be very misleading to measure the system noise level at high frequencies without any applied modulation to the laser, and then to calculate the anticipated S/N ratio based on these measurements, as if the signal and the noise are independent entities.

It should be noted that a similar translation of low frequency noise onto the high frequency modulation carrier also exists for systems using diode-pumped YAG lasers with external modulators.

The low frequency noise, from the diode-pumped YAG laser, typically below tens of megahertz, originates from relaxation oscillation and from beating between longitudinal modes, the latter being very significant even with an excellent side-mode rejection. These low frequency noises must be rid of by feedback using an additional modulator.

For single frequency lasers such as DFB lasers, neither mode-partition nor mode-hopping noises become much of an issue. The dominant source of low frequency noise comes from double reflections along the fiber length which serves to convert the laser phase noise to intensity noise[15,16,5]. With the use of good optical connectors, reflections along the link can be minimized except for intrinsic Rayleigh back-scattering[17]. The resulting intensity noise spectrum is basically that of the (Lorentzian) laser lineshape centered at DC, with a typical linewidth of a few tens of megahertz. On applying high frequency modulation this noise will be translated along with the modulation carrier. In generally, this effect is much less than that of FP lasers, provided proper optical connectors and splices are employed. These parameters will again be quantified later.

To illustrate the effects discussed above, we first show measured results for links consisting of a 1.3μm (a) FP laser and (b) DFB laser, modulated at frequencies of 6.5GHz and 10GHz, propagating through a distance of 1km, 6km and 20km of single mode fibers. Both of these are high speed lasers with a 3dB modulation bandwidth of well beyond 10GHz, as shown in Fig. 5(a). A single high speed pin photoreceiver with a 12GHz 3dB bandwidth is used for all of the measurements. The spectra of the lasers are shown in Fig. 5(b) and (c). The measurements are done with an input RF drive level into the lasers at +10dBm. As a point of reference, the 1dB compression level of the laser is +15dBm. The optical input into the photoreceiver are adjusted to give 1mA of DC photocurrent in all cases, except where noted in a few instances. Angled polished optical connectors (APC) are used whenever a connection is required, which amounts to between 2-4 pairs of connectors for the links used in this experiment.

For the FP laser, low frequency mode-partition noise can be clearly observed on propagation through only a few kilometers of fibers, as shown in Fig. 6(a) and (b). The highest of these noise levels correspond to RIN figures of <-145dB/Hz[1] with no fiber, -132dB/Hz after propagating through 6km, and -115dB/Hz after 20km. In contrast, for the DFB laser the noise spectrum is at the receiver noise limit of <145dB/Hz at 6km (Fig. 7a), and remains to be so after 20km (Fig. 7b). Nevertheless, at 20km one can already observe a hint of the interferometric noise protruding above the receiver noise level at low frequencies (Fig. 7b). This low level of interferometric noise is due to Rayleigh scattering of a long piece of fiber and reflection from the APC connectors. The nature of the interferometric noise can be much easily observed when bad splices or connectors exist in the link, as illustrate in Fig. 7(c) - a situation clearly to be avoided.

The kind of low frequency noises described above are quite commonly observed in typical fiber links. In the following, we illustrate how the low frequency noises are translated to the neighborhood of the modulation carrier upon applying a direct high frequency direct modulation to the laser. Figure 8 shows the result of applying a 6.5GHz modulation carrier to the FP ((a)-(c)) and the DFB lasers ((d)-(f)), and observed after transmission through 1km, 6km and 20km. The blanks in the traces for FP lasers in Fig. 8(a)-(c) establish the RIN level with the RF drive to the laser disconnected, i.e., without noise translation. These plots illustrate that the low frequency noise and its translation is very significant. The drop in the RF signal level at longer fiber lengths for the FP laser (Fig. 8c) is due to fiber dispersion but not attenuation (recall that all measurements, except where noted, are done with 1mA of photocurrent from the receiver.) One should contrast the above results with those obtained with the DFB laser, Fig. 8(d)-(f). Only at 20km does the translated noise becomes slightly visible, consistent with the low frequency noise observations of Fig. 7.

All of the above observations hold for modulation at 10GHz, as shown in Fig. 9(a)-(f), except for the even more striking difference between the FP laser (Fig. 9(a)-(c)) and the DFB laser (Fig. 9(d)-(f)). It is worthwhile to note that for a DFB laser, only a very slight degradation is observed even at 10GHz and at 20km, while the FP laser is all but unfunctional at these frequencies and

---

1 This number is receiver noise limited.

distances. Note also from Fig. 8(b) and 9(b) that even at a relatively short distance of 6km, the actual S/N ratio of the high speed FP laser is, depending on the modulation frequency, between 10-20dB worse than that predicted from a standard RIN measurement alone (without modulation applied).

2.2 Modulation efficiency

2.2.1 Gain lever

Gain-lever is an effect which ultilizes the highly sublinear nature of the quantum well gain characteristic to accomplish very high modulation efficiencies in intensity modulation (IM) and frequency modulation (FM), as well as broad wavelength tunability[18,19]. To appreciate the gain lever effect, consider a single quantum well laser which has a typical gain charactersitic as shown in Fig. 10 and which is inhomogeneously pumped in a tandem contact geometry. The principle of operation is as follow: when the device is above lasing threshold, the sum of the optical gain of the sections is clamped at a constant value (equal to the cavity loss). If one section increases in optical gain by, say, injection of extra electrons, then the other section must automatically reduces its gain by the same amount by ejecting the extra electrons. If each section is pumped by a constant current source, then the extra electrons cannot be ejected electrically but will do so optically through the emission of photons. According to Fig. 10, when the sections are biased as shown, then a small modulation applied to section "a" will result in a large modulation in the optical output by the "levering" effect.

Quantitatively, the modulation performance of this device is described by the rate equations:

$$\dot{S} = S\left(\Gamma G_a(1-h) + \Gamma G_b h - \frac{1}{\tau_p}\right) \tag{13a}$$

$$\dot{N}_a = \frac{J_a}{ed} - BN_a^2 - G_a S \tag{13b}$$

$$\dot{N}_b = \frac{J_b}{ed} - BN_b^2 - G_b S \tag{13c}$$

where S, $N_{a,b}$, $J_{a,b}$, $G_{a,b}$ are the photon density, carrier densities, injection currents and optical

gain in the respective sections; Γ is the optical confinement factor; h is the fractional length of the gain section, and a bimolecular recombination is used which is shown experimentally to be appropriate for quantum well structures[20]. A small signal analysis yields the desired expression for the photon density modulation amplitude $s$shown in Fig. 11. It can be shown that[18,21] the relative modulation efficiency at frequencies below relaxation oscillation is

$$\eta = \frac{\gamma_b}{\gamma_a} k \tag{14}$$

valid for h approximately equal to 1. At low optical power, the spontaneous lifetimes dominates and $\gamma_b \cong \gamma_a$. The enhancement in modulation efficiency is thus approximately equal to the ratio of the slopes of the differential gain. At high optical power the stimulated lifetime dominates and $\gamma_b / \gamma_a \cong 1/k$. Because of a shorter stimulated lifetime in the modulation section, a larger modulation current is needed to produce the same amount of modulation in the electron density, thus reducing the effectiveness of the levering effect. In fact, at a sufficiently high optical power, the levering effect is completely neutralized and the modulation efficienty is no diferent from that of a uniformly pumped device. This implies a limited modulation bandwidth for gain lever lasers, unless for those with a very short photon lifetime (cavity length).

The gain-lever effect has been experimentally demonstrated first by optical modulation[18] and then by electrical modulation[19]. An example of the latter is shown in Fig. 12. The laser bandwidth is between 3 and 6GHz at output power levels up to 4mW for this particular device under uniform injection, as shown by curves labelled "uniform" in Fig. 12(a) for a 220μm device. The two sections are then biased separately, with the bias current into the modulation section reduced and that into the gain section increased correspondingly to keep the output power constant. The relaxation oscillation frequency remains essentially unchanged. Microwave modulation is applied to the modulation section whose gain is estimated to be 0.2 that of threshold gain. The modulation responses are plotted in Fig. 12 as shown by curves labelled "tandem". The improvement for lower f_r and for shorter devices are evident. The largest improvement observed was about 23dB, with the 220μm device at $f_r \cong$ 3GHz.

Based on the current understanding of the gain-lever effect, it is not expected that the modulation bandwidth of the gain-lever transmitter can much exceed 10GHz. For millimeter wave frequency systems operating at 50GHz and above, alternate system architectures must be deviced. Since radar signals are intrinsically narrowband signals of at most a few GHz, (although the carrier frequency can hop around for anti-jamming), one can consider narrowband impedance matching as a means of enhancing the modulation efficiency, and hence the Noise Figure, of laser diode links. This is the subject of the following section.

2.2.2 Impedance matching

A primary reason for using fiber-optics for microwave transmission is the very low loss of optical fibers at below 1dB/km, as compared to coaxial cables of dB's/100ft. This type of comparison does not take into account the losses encountered in the electrical-to-optical-to-electrical convertion and in launching the laser radiation into and out of the optical fiber. If we take some typical numbers for the efficiencies of state-of-the-art lasers and detectors: 0.25mW/mA for 1.3μm laser and 0.65mA/mW for pin detectors, and assuming 30% laser-to-fiber coupling and 95% fiber to detector coupling, then the end-to-end signal throughput suffers a loss of 27dB. It is interesting to note that from this point onward, each additional km of transmission adds only a fraction of a dB to the signal loss, so that for any appreciable distance (>100m) fiber links are almost always superior to coaxial links. Nonetheless, if this throughput loss can be made to be minimal or even zero, it would eliminate the need for an active amplifier following the photodiode, and make fiber optics attractive even to applications requiring short distances.

To reduce the throughput loss one must improve on the efficiencies of all the components involved. It would probably be quite difficult to improve significantly on the intrinsic efficiencies of the laser and detector without major breakthroughs in device technology. However, the external efficiency of the laser can be improved by roughly a factor of two by applying antireflection coating to the back facet. The laser-fiber coupling is primarily a package problem made quite difficult by thermal and shock requirements and other military specifications. Nevertheless, one can expect

coupling efficiencies of around 50% to be achieved routinely with a production line process which conforms to military specifications. These improvements will bring the throughput loss down to about 16dB.

The next area for throughput enhancement is in impedance matching of the laser and photodiode. At microwave frequencies one is expected to work in a 50Ω system. A forward biased diode presents an impedance of about 5Ω, and a 45Ω chip resistor is customarily place in series with the laser diode for broadband impedance matching. The photodiode is basically a high impedance current source and is launched directly into a 50Ω line without any special matching. These schemes provide very simple yet effective, broadband, matching but is not optimized for efficiency. Consider the laser matching problem: if a lossless impedance matching network is placed between the 50Ω source driver and the laser diode as in Fig. 13a, such that the combined matching network and the laser diode presents a perfect 50Ω to the source, all the power delivered from the source must be absorbed by the resistive part of the laser diode, in which case the current gain over that of broadband resistive matching is $(50/R)^{1/2}$. For R=5Ω, a gain of 10dB is achieved for a perfect match, in which case the throughput loss will be reduced to only 6dB. The procedure of synthesizing the matching network can be found in many standard textbooks [22]. The actual circuit design will not be discussed here, rather we shall discuss some of the fundamental limitations as far as matching bandwidth is concerned.

The type of lossless matching described above must necessarily be narrowband, from a network theorm first derived by Bode[23] for a simple RC network and later expanded by Fano[24] and others to any circuit. For a RC network, the following gain-bandwidth relationship applies:

$$\int_0^\infty \ln\left|\frac{1}{\Gamma}\right| d\omega = \frac{\pi}{RC} \qquad (15)$$

where Γ is the reflection coefficient of the combined impedance matching network and the load (the laser). For a perfect match, Γ=0 and throughput efficiency will attain the theoretical gain descibed above. If good matching is desired for the frequency range of f_a to f_b, the best result will be obtained

when $\Gamma \approx 1$ at all frequencies (i.e., perfect mismatch) outside the band. In this case, assuming Γ to be constant inside the band, Eq. (15) gives

$$|\Gamma| = e^{-\pi f_0/\Delta\omega} \tag{16}$$

where $\Delta\omega = 2\pi(f_a - f_b)$ and $f_o = 1/RC$. This represents a gain in throughput efficiency (over that of wideband resistive matching) of

$$G = 10\log\frac{50}{R}(1 - e^{-\pi f_0/\Delta f}) \tag{17}$$

The ideal "square" passband described above can be approached by using higher order network of various types, the choice of which will depends on the design complexity and ripple requirements within the pass band. Fig. 13b plots G against $RC\Delta f$, which is the matching bandwidth as a fraction of the RC bandwidth of the laser, according to Eq. 17, and assuming $R = 5\Omega$ typical of a laser diode. A significant observation from this plot is that near perfect matching can be accomplished for $RC\Delta f \rightarrow 1$, which means that matching can be accomplished without much sacrifice in the laser bandwidth as limited by the parasitic RC . It is obvious that further gain can be obtained if the laser resistance can be lowered.

Although photodiodes are not a subject of study in this contract, it is appropriate to point out here that significant gain can be obtained by proper impedance matching of the photodiode. The photodiode can be modelled as a high impedance current source shunted by a parallel capacitor. A simple receiver can be implemented by launching the photodiode current directly into a 50Ω load. An impedance matching network placed between the photodiode and the load as in Fig. 16 can lead to a voltage gain F with the following gain-bandwidth product limitation:

$$\int_0^\infty F(\omega)d\omega = \frac{\pi}{2CR_L} \tag{18}$$

The impedance matching amounts to creating a network, with the parasitic capacitance and the load resistance as part of the circuit components, which presents a high impedance to the current source over a specific frequency band. By reducing the detector bandwidth four-fold, the remaining 6dB of throughput loss as discussed in the previous part of this section can be overcomed. Further reduction in bandwidth can lead to overall throughput gain.

3. Narrowband millimeter wave modulation by photomixing and feedforward compensation.

Over the past few years, attempts have been made to generate the microwave or millimeter wave signals themselves directly from mixing two laser beams. The signal frequency can be varies very easily and broadly by tuning the optical frequencies. One must, however, realize that the mere ability to generate a microwave tone is very far from the ability to transmit a microwave signal that has some intelligent content. Furthermore, the laser linewidth and the absolute lasing frequency - both of which are very sensitive quantities - must be controlled very accurately in order for the resultant microwave signal to be of decent quality (by RF standard).

We investigate a microwave/millimeter wave optical modulation technique module based on optical mixing but which do not require accurate control of lasing frequencies and stability. The modulation bandwidth, on the order of 3-5GHz, will be centered at a frequency that is tunable from 20GHz to 100GHz. The signal quality and achievable S/N ratio will be studied and compared to existing techniques currently available at lower frequencies.

The technique is based on a feedforward control of the microwave signal generated from mixing two single-frequency laser beams. Two distributed feedback semiconductor lasers (DFB) are used. Since the wavelength of the two lasers can be tuned separately from each other, either thermally or through the injection current, the beat frequency can be tuned over a wide range of several hundred GHz. The linewidth of the beat note is, however, on the order of 30MHz, which is unacceptable for any microwave applications. Currently, it is very difficult to narrow down this linewidth without resorting to special (and hence unproven in reliability) laser structures and/or sensitive external cavity controls. Furthermore, a way has to be found to modulated the input signal on the optical beam. We use the scheme shown in Fig. 14 to accomplish these tasks. Here, two 1.3μm DFB lasers are combined in a fiber optic directional coupler (the polarization controller allows for the alignment of the relative polarization of the tow lasers at the coupler) to produce two outputs, each with an intensity beat note at the laser difference frequency. One of the outputs form the coupler is detected and the beat signal is mixed with the input signal, which we intend to transmit down the link. The down-converted signal (at a frequency equal to the difference the input signal

and the beat note) is filtered, amplified and sent to an $LiNbO_3$ external modulator with a readily achievable modulation bandwidth of 5-10GHz. The external modulator performs the function of mixing the down converted signal with the beat note, with the resultant signal in optical form. Thus, any difference between the input signal and the beat note is fed forward to the external modulator which corrects the beat note, resulting in the emergence of the original input signal modulated on an optical beam, regardless of the precise frequency and the "noisiness" of the beat note. This technique requires the exact matching of the delay between the feedforward path and the original optical path (see Fig. 14).

This technique can be thought of as a way to extend the low frequency modulator to high frequency, narrow band operation. The modulator sees only the low frequency, down-converted error signal, and does not need to respond t the high frequency of the input signal. The frequency band of operation is determined by the beat note, which means that by controlling the frequency of the beat note, different frequency bands can be selected.

3.1 Theory of operation

Refering to Fig. 14, the output of two 1.3 micron Distributed Feedback (DFB) lasers are combined in a fiber-optic directional coupler (the polarization controller allows us to align the polarizations of the two lasers at the coupler) to produce two outputs each with an intensity beat note at the laser difference frequency. One of the outputs from the coupler is detected and the beat signal is mixed with the input signal which we intend to transmit over the link. The down converted signal (at a frequency equal to the difference between the input signal and the beat note) is filtered, amplified and sent to a $LiNbO_3$ external modulator. The external modulator mixes the down converted signal with the beat note so that the input signal is recreated on the optical carrier. Assuming the modulator is operating in the linear region, its output can be expressed as

$$I_{out} = I_{in}(q_1 - kmq_2/2) \tag{19a}$$

where

$$q_1 = 1 + kcos[\omega_b t + \varphi(t)] - mcos[(\omega_{in} - \omega_b)t + \varphi(t+\tau)] \tag{19b}$$

$$q_2 = cos[(2\omega_b - \omega_{in})t + \varphi(t+\tau) + \varphi(t)] + cos[\omega_{in}t + \varphi(t) - \varphi(t+\tau)] \tag{19c}$$

and where the symbols have the following meaning

I_{in} - input intensity

k - modulation index of laser beat note

m - modulation index achieved by the down converted mixer product driving the modulator

$\varphi(t)$ - time dependent phase of laser beat note

τ - difference in time delay for the two paths from the coupler to the modulator

ω_b - laser beat note frequency

ω_{in} - input frequency

The intensity spectrum has four components: the beat frequency, ω_b, the down converted beat frequency, $\omega_b - \omega_{in}$, a mixer product at $2\omega_b - \omega_{in}$ and a replica of the input signal, ω_{in}.

Note that when the time delay, τ, is zero, the phase noise cancels for the component at ω_{in}. This can be verified through a more complete analysis. Assuming the phase noise of the laser beat note to have a Gaussian distribution with a coherence time, t_b(i.e. the laser beatnote is Lorentzian with a full-width-at-half-maximum linewidth of $1/\pi t_b$), we find the following power spectrum for the replica of the input signal

$$S(\omega) = 2\pi e^{-|\tau|/t_b}\delta(\omega) + 2t_b/(\omega^2 t_b^2 + 1)(1 - ((|\tau|/t_b)(sin(\omega|\tau|))/(\omega|\tau|) - cos(\omega|\tau|))e^{-|\tau|/t_b}) \quad (20)$$

where ω is the frequency offset from ω_{in}. As expected from Eq. 19, this expression simplifies to a delta function when τ=0.

To determine the achievable signal-to-noise ratio for the optical up-converter, we must consider the traditional noise sources common to all fiber-optic links. These are the laser relative intensity noise (RIN), the shot noise and the thermal noise in the receiver. In addition, the replica of the input signal will have noise side bands due to imperfect matching of the time delays of the electrical and optical paths, and the noise sidebands of the beatnote, which is separated from the signal by the maximum frequency of the modulator, will extend into the signal band. Consider now a typical system where the laser RIN is 150 dB, the photo current is 1 mA, the receiver resistance is 50 ohm and the modulation indices, k and m, equals 1 and 0.5 respectively. The signal-to-noise ratio (S/N) of this system is limited to 138 dB/Hz by the RIN (the 12 dB degradation is due to the factor $km/2$ in Eq. 19) and 143 dB/Hz by the thermal and shot noise. The S/N of 138 dB/Hz will therefore serve as a baseline when evaluating the influence of the non-traditional noise sources. Noise in the electrical path need not be considered if the detector photocurrent in the electrical path is large enough to let the laser noise dominate over the thermal noise. Under these conditions, the S/N is the full RIN of the laser, because the reducing factor km/2 is not applicable, and the mixer and amplifier add little to the noise (the noise figures of these components are not valid because the noise is much larger than the thermal noise limit). The noise at the output of the optical up-converter is therefore dominated by the noise in the optical path.

The noise due to imperfect matching of the time delay is given by Eq. 15. The line width of the laser beatnote is typically on the order of 25 MHz, which means that the coherence time is roughly 13 ns. Both in an opto-electronic integrated circuit (OEIC) and a bulk fiber-optic embodiment of the up-converter, it is reasonable to assume that the delay can be controlled to better than 1 ps, which corresponds to a path length of 200 μm in a silica waveguide. We therefore have $|\tau| << t_b$. Further, the signal bandwidth will be limited to a few GHz, so $\omega|\tau| << 1$. Using these relationships, Eq. 20 can be simplified significantly

$$S(\omega) = 2\pi\delta(\omega) + |\tau|^2/t_b \tag{21}$$

Note that under the above assumptions, the noise is not a function of the frequency offset! The S/N is then simply given by $2\pi t_b/|\tau|^2$. With a delay of 1 ps, and a coherence time of 13 ns, this evaluates to 169 dB/Hz regardless of bandwidth. In a narrow band this is better than the best available electrical signal generators, and in a wide bandwidth it is better than the laser RIN. If the delay difference can be controlled to a 1 ps accuracy, the noise sidebands of the signal are therefore negligible.

The second noise source that is special to the optical up-converter is the noise from the nearby laser beatnote, i.e. the term $kcos[\omega_b t + \varphi(t)]$ in Eq. 19 (the other terms are further away from the signal band and therefore less important). The S/N due to this term is given roughly by

$$S/N = (m^2\omega_d^2 t_b)/4B \tag{22}$$

where B is the bandwidth and ω_d is the difference between the laser beatnote frequency and the signal frequency. This difference frequency roughly equals the operating frequency of the modulator. Assuming a value of 5 GHz for the frequency difference, a modulation index of 0.5 and a coherence time of 13 ns, the S/N is 119 dB/Hz. We see that with these reasonable assumptions on laser and modulator performance, the noise from the laser beatnote dominates all other noise sources in the system. To make matters worse, it is well known that the laser linewidth, and therefore the beatnote intensity spectrum, do not follow a Lorentzian distribution far from the

line center, but has additional noise peaks separated from the center by the relaxation oscillation frequency. Typical DFB lasers have their relaxation frequency in the 5 to 10 GHz range under normal operating conditions. If the frequency difference of the signal and the laser beatnote is in the same range, this will lead to a further decrease of the S/N.

3.2 Experiment

The experiment shown schematically in Fig. 14 was carried out using two standard, commercial 1.3μm DFB lasers. Thermo-electric coolers were used to stablize and control the temperature of the lasers. Pairs of lasers were used so that they were close in lasing frequency (¡50GHz) when operated at the same temperature and current. The stability was best when the lasers were operated no more than a few degrees of room temperature, but with a sensitivity of 12GHz/deg, the tuning range was at least 13GHz. The local oscillator frequency was tunable to 8GHz and the low pass filter after the mixer had a 1GHz bandwidth (the modulator bandwidth exceeds this). A variable delay was inserted in the electrical path in front of the modulator.

Figure 16 shows a typical intensity spectrum for the modulated light. All four frequency components from Eq. 19 can be identified. The delay is adjusted to maximize the LO signal component. An expanded view of the RF spectrum in the vicinity of the signal is shown in Fig. 17, for the relative delay adjusted to 0ns, 7ns and 23ns. As the relative delay is increased, the signal to noise ratio is reduced according to Eq. (22). These results are in excellent agreement with theory.

At this time we are in the process of demonstrating millimeter wave transmission at 40GHz using the same technique. A better S/N ratio is also sought after by optimization of parameters.

3.3 Optimization of parameters

According to Eq. 22, the noise from the laser beatnote can be reduced by increasing the difference frequency, ω_d, and by increasing the laser beatnote coherence time, t_b. By increasing the modulator bandwidth to 20 GHz, the S/N is increased by 12 dB. Using DFB lasers with

linewidths on the order of 1 MHz, corresponding roughly to a beatnote width of 2 MHz and a coherence time of 160 ns, adds another 11 dB to the S/N. With these improvements, we see that the S/N due to the beatnote sidebands becomes 142 dB/Hz, i.e. better than the S/N due to the laser RIN. The optimum laser structure should also have a relatively low relaxation oscillation frequency, so that the noise 10 to 20 GHz away from the line center is equal to or less than that predicted by the Lorentzian distribution. As an alternative to increasing the S/N by using improved modulators and lasers, the beatnote noise can be suppressed by a transversal filter, which is an optical waveguide component that can relatively easily be incorporated in our design.

The distortion in the optical up-converter is determined by the distortion in the modulator that is employed. In general, most high-speed modulators, and specifically the one we plan to use in our experiments, are based on an interferometric conversion of phase to intensity modulation which results in a (co)sine dependence of the output intensity on the driving voltage. Schemes for compensation of distortions in such type of modulators are well known and can be easily applied.

It appears that proper choice of lasers is essential for the optical modulation scheme described here. The important considerations will be stability, tunability and the suppression of side peaks in the intensity spectrum. Following a theoretical analysis to establish the optimum structures for our application, we will obtain the commercially available lasers that most closely matches our chosen design. Using these lasers we should be able to build an up-converter, tunable up to 60 GHz, with an improved S/N. The system will first be implemented in bulk fiber optics, while a OEIC version will be built if the funding is available.

If a laser structure with sufficiently low phase noise cannot be developed, a transversal filter will be used to suppress the laser beatnote noise. Transversal filters are ideal for signal processing of microwave signals on optical carriers, and are easily implemented in the same bulk fiber optic and OEIC technologies that we are considering for the feed forward modulator, and will therefore not lead to a too large increase of the overall complexity of the system. The most

challenging part of incorporating a transversal filter in the optical path, is to do so without adversely affecting the tunability of the feed forward modulator.

4.0 Conclusion

We have, in this contract, examined some of the systems issues concerning fiber-optic applications in microwave systems, specifically, that in phased array systems. The two key problems we chose to examine are Noise Figure of the link, and the problem of modulation a high frequency (millimeter wave) signal on an optical carrier without the availability of directly modulatable sources at those frequencies. The Noise Figure problem was tackled by increasing the modulation efficiency and reducing noise. The modulation efficiency can be increased by the quantum well gain-lever effect or by proper impedance matching. The former operates at frequencies at below a few GHz, while the latter is applicable at higher frequencies. The noise issue is examined, apart from its obvious reduction through the use of higher power lasers, from the perspective of mode-partition noise and noise translation, as well as noise induced by fiber reflections including those due to Rayleigh scattering. On the second problem of optical modulation at millimeter wave frequencies, we have developed an innovative method that uses the beat signal between two (relatively noise and unstable) lasers, and using feedforward to correct for it and to impress the modulation signal on top of it. This technique looks very promising and considerable improvements above the present performance can be obtained by proper optimization of parameters. It is highly likely that continued development in this area can lead to the first practical millimeter wave modulatable optical light source for use in systems demonstrations in the near future.

References

1. K. Sato, IEEE J. Quant. Electron., **QE-19**, 1380-1391 (83).
2. K. Vahala and A. Yariv, Phys. Rev., (86).
3. K. Vahala and A. Yariv, IEEE J. Quant. Electron., **QE-19**, 1096-1101, 1102-1109 (83).
4. C.H. Henry, IEEE J. Quant. Electron., **QE-18**, 259-264 (82).
5. K. Petermann, **Laser diode modulation and noise**, Kluwer Academic Publishers, 1988.
6. C.B. Su, J. Schlafer and R.B. Lauer, Appl. Phys. Lett., **57**, 849-851, 1990.
7. C.H. Henry, J. Lightwave Tech., **LT-4**, 288 (1986).
8. K.Y. Lau and A. Yariv, Appl. Phys. Lett, **45**, 1034-1036 (84).
9. L.F. Lester, S.S. Keefe, W.J. Schaff and L. Eastman, Electron. Lett., **28**, 383-385, 1992.
10. R. Nagarajan, T. Fukushima, J. Bowers, R. Geels and L. Coldren, Appl. Phys. Lett., **58**, 2326-2328, 1991.
11. K. Uomi, H. Nakano and N. Chinone, Electron. Lett., **25**, 668-669 (1989).
12. M. Yamada, IEEE J. Quant. Electron., **QE-22**, 1052-1059, 1986.
13. G.J. Meslener, Photonic Tech. Letters.
14. K.Y. Lau and H. Blauvelt, Appl. Phys. Lett., **52**, 694-696, 1988.
15. M.M. Choy, J.L. Gimlett, R. Welter, L.G. Kazovsky and N.K. Cheung, Electron. Lett., **23**, 1151-1152, 1987.
16. J.L. Gimlett and N.K. Cheung, IEEE J. Lightwave Tech., **7**, 888-895, 1989.
17. S.W. Wu, A. Yariv, H. Blauvelt and N. Kwong, Appl. Phys. Lett., **59**, 1156-1158 (1991).
18. Vahala K.J., M.A. Newkirk and T.R. Chen, Appl. Phys. Lett., **54**, 2506 (1989).
19. Moore N. and K.Y. Lau, Appl. Phys. Lett., **55**, 936 (1989).
20. Arakawa Y., H. Sakaki, M. Nishioka, J. Yoshino and T. Kamiya, Appl. Phys. Lett., **46**, 519 (1985).
21. K.Y. Lau, IEEE Photonics Tech. Lett., **3**, 557 (1991).

22. G. Matthaei, L. Young and E.M.T. Jones, **Microwave filters, impedance matching networks and coupling structures**, Artech House 1980.

23. H.W. Bode, **Network analysis and feedback amplifier design**, pg. 306, Van Nostrand 1947.

24. Arakawa Y., K. Vahala and A. Yariv, Appl. Phys. Lett., 45, 950 (1990).

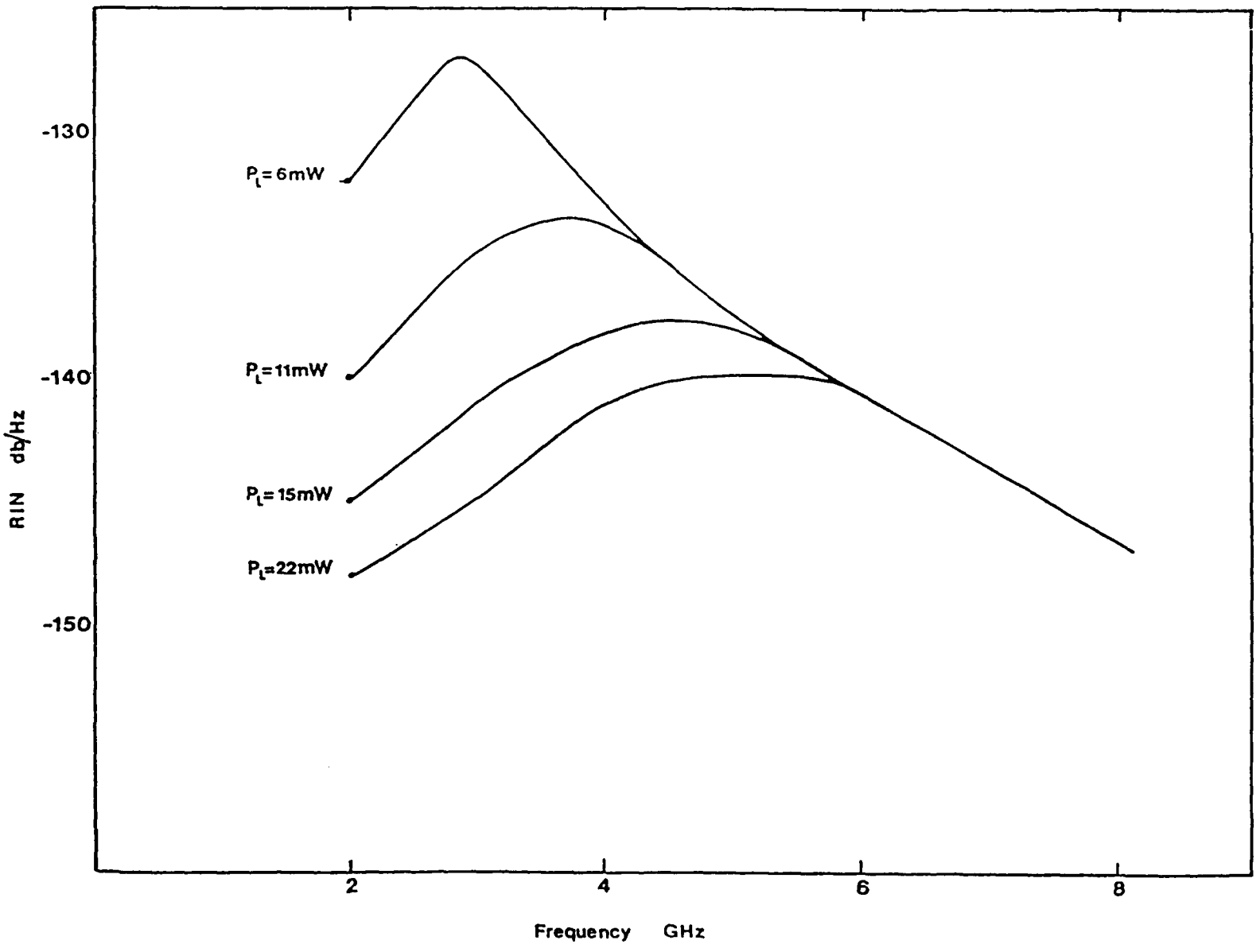

Fig. 1 Typical measured RIN spectrum of 1.3μ DFB lasers.

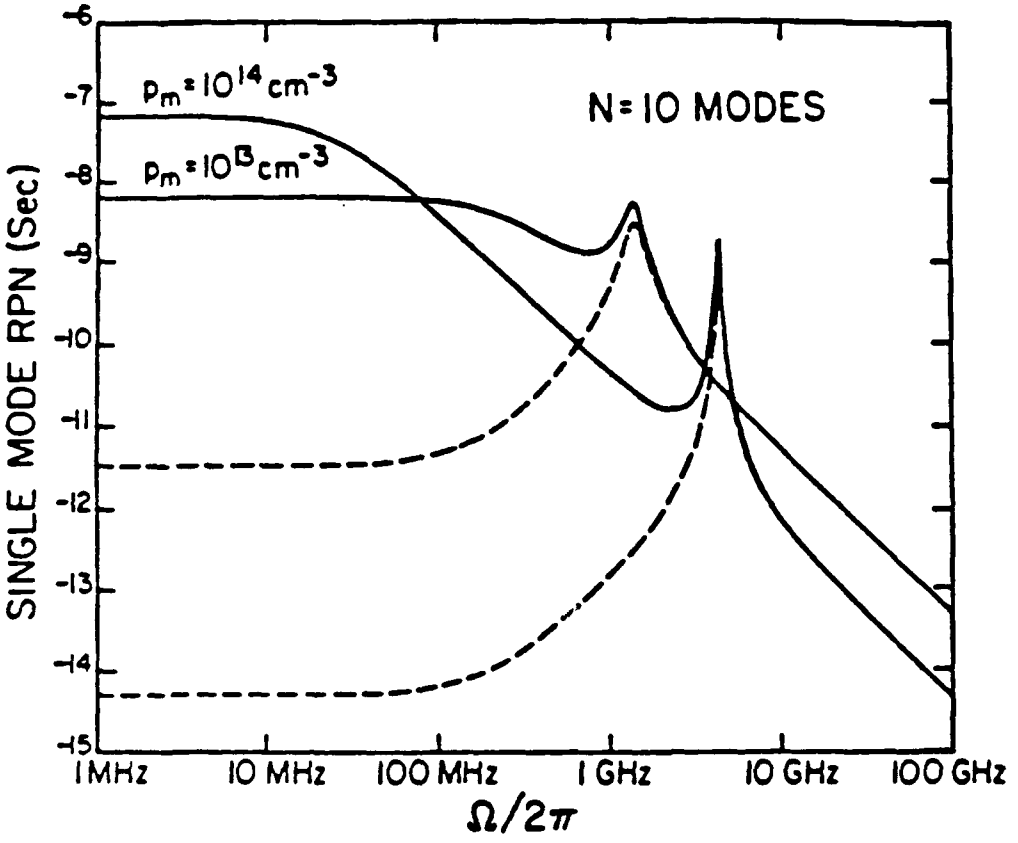

Fig. 2 Calculated mode-partition noise with 10 modes

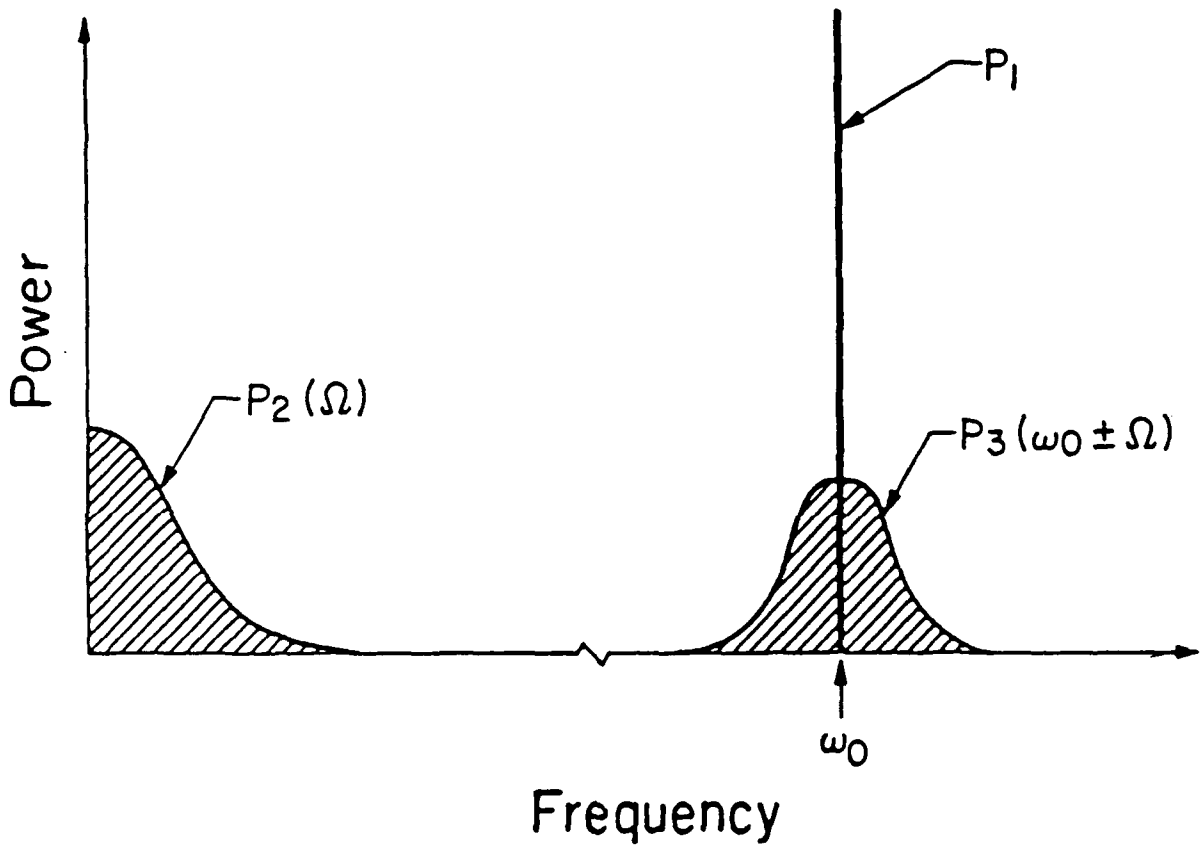

Fig. 3 Schematic representation of the various noise spectra used in calculating the translation factor of low frequency noise to high frequencies by intermodulation.

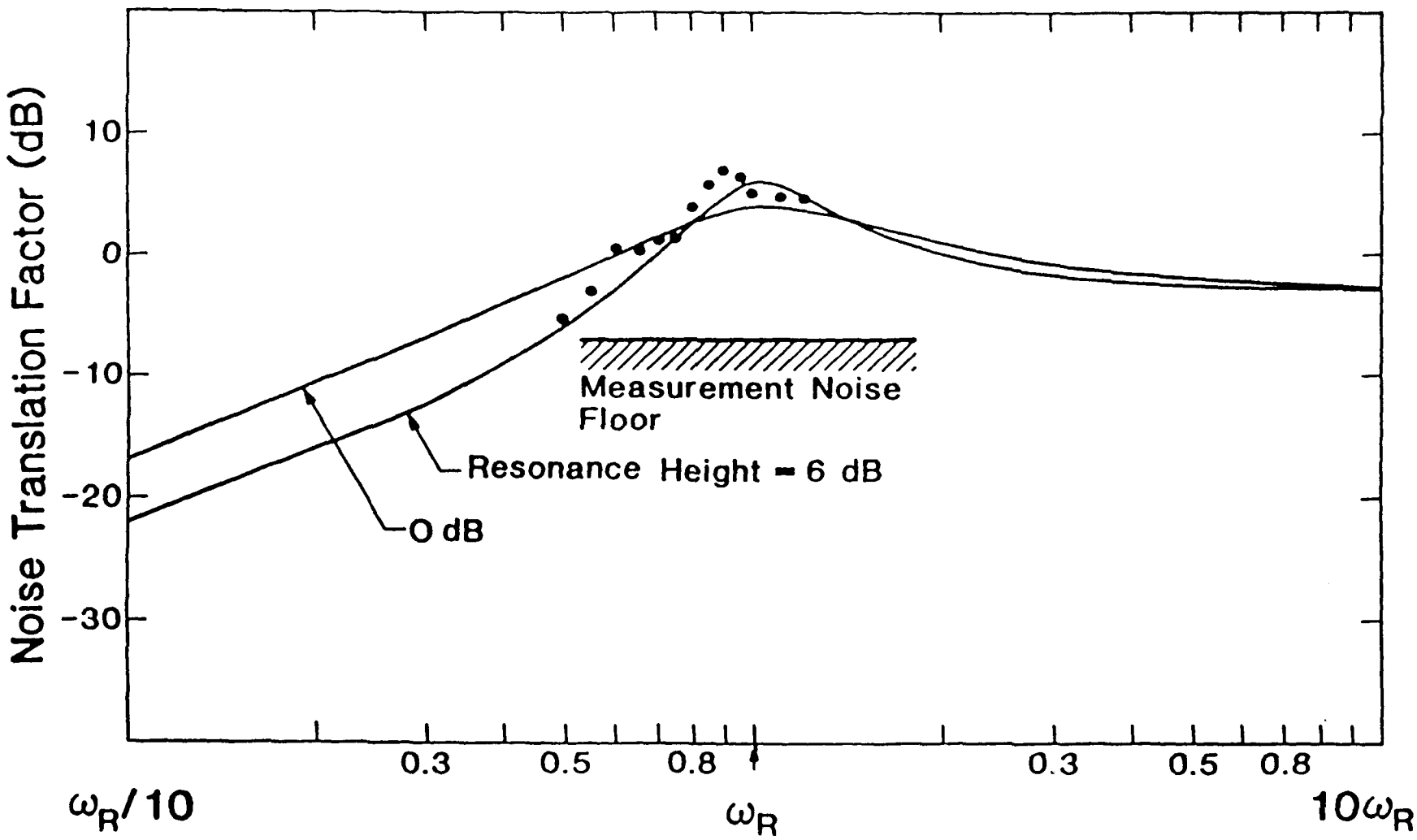

Fig. 4 Low frequency noise translation factor.

Fig. 5 (a) Direct modulation response of the high speed FP and DFB lasers used in this experiment. Both lasers has an estimated relaxation oscillation frequency at slightly below 10GHz, although the resonances of the both lasers are strongly damped.

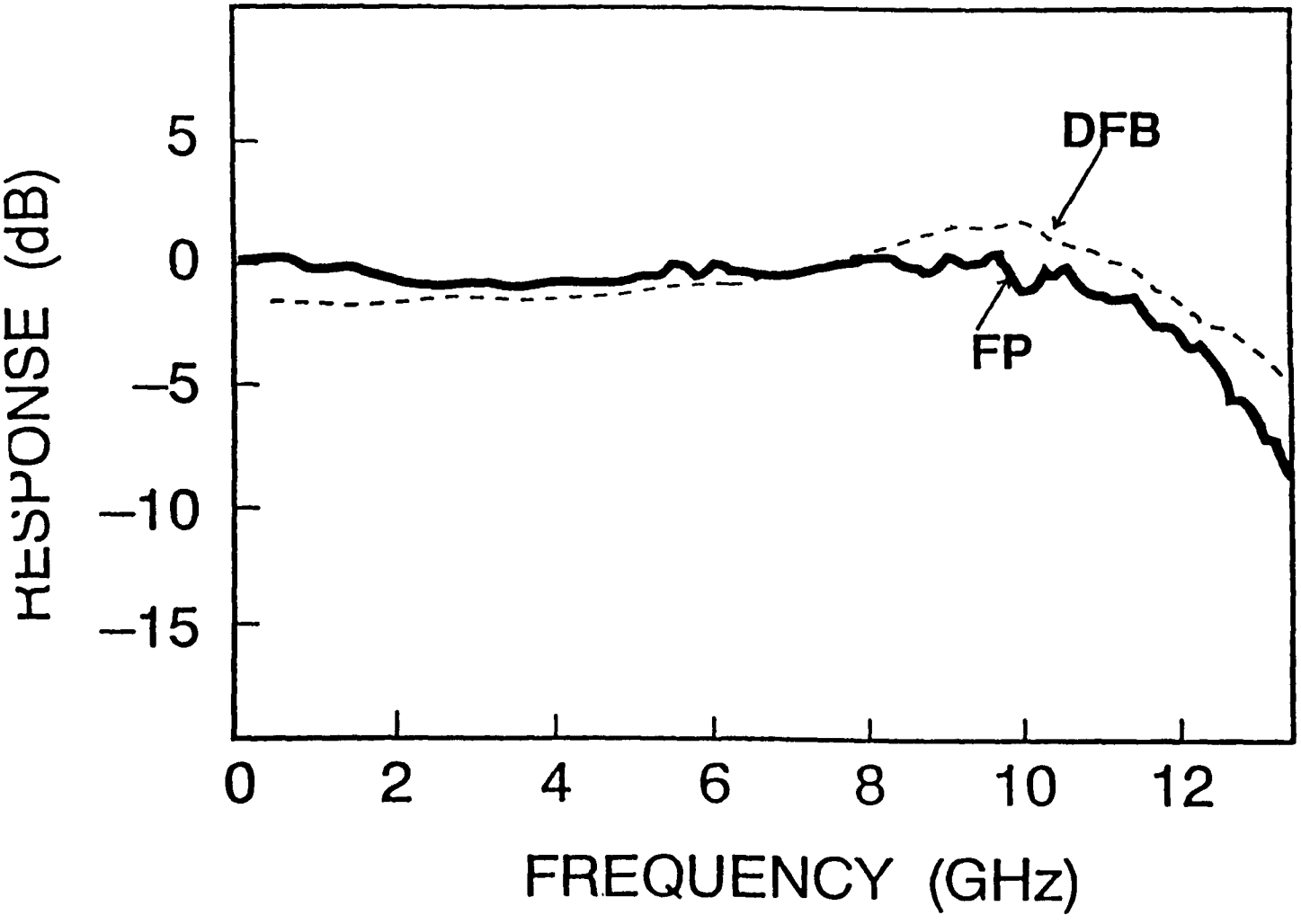

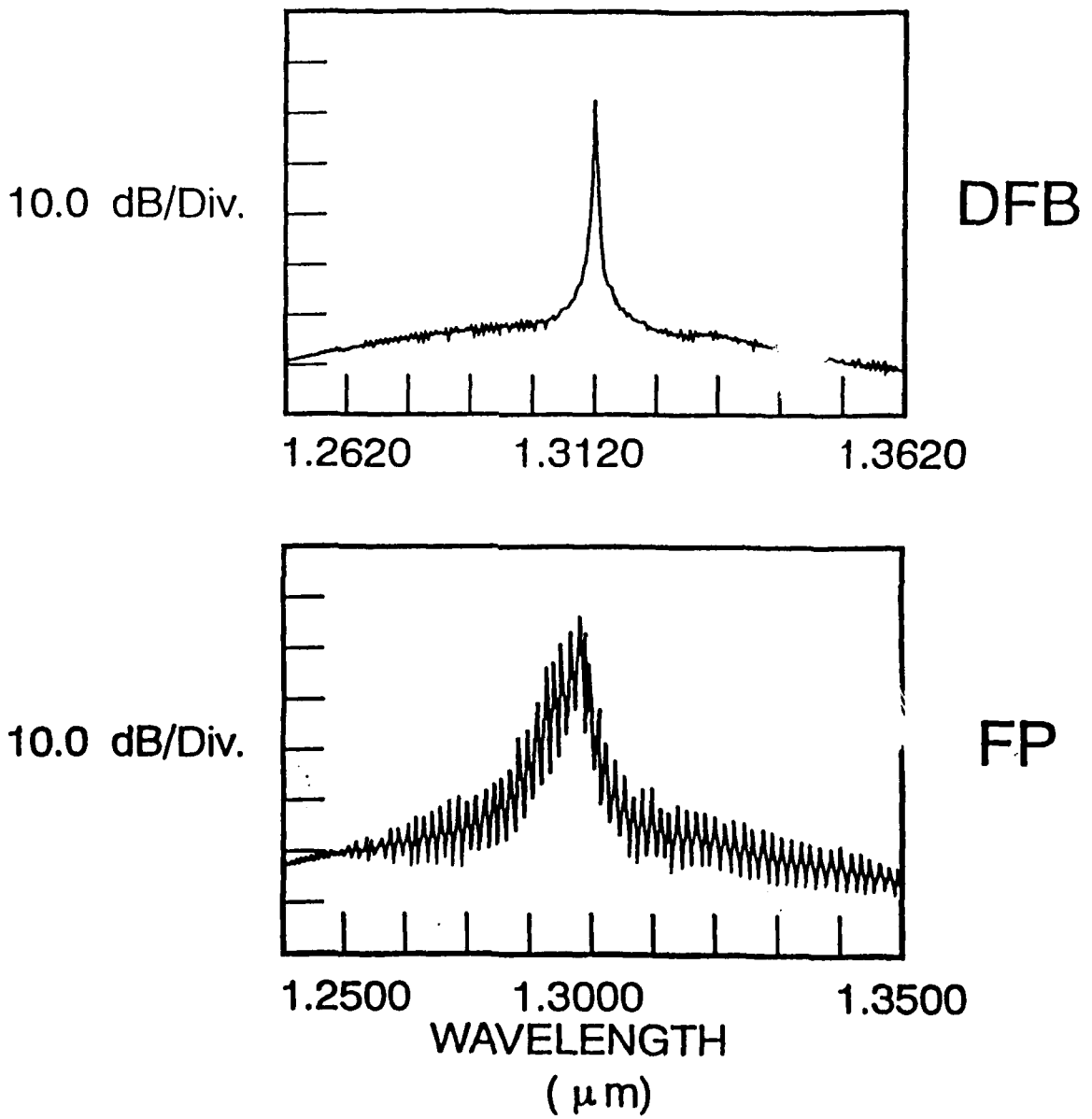

Fig. 5 (b) and (c) - lasing spectrum of the FP and DFB lasers, respectively.

Fig. 6 Mode partition noise in FP lasers after transmission through (a) 6km and (b) 20km of single mode fibers.

6 km

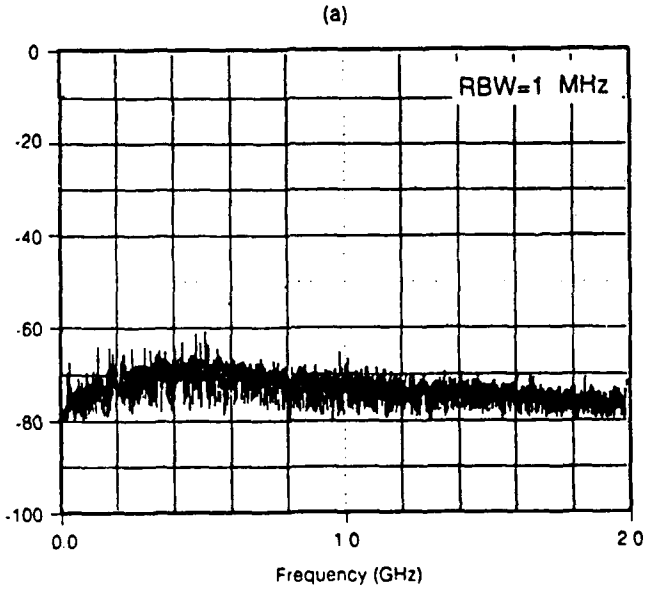

20 km

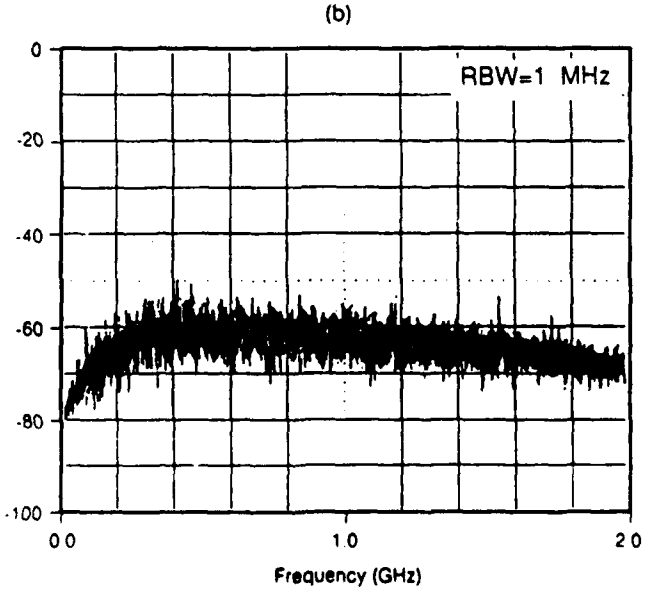

Fig. 7 Interferometric phase→intensity converted noise for DFB lasers due to double Rayleigh scattering, for transmission through (a) 6km and (b) 20km of single mode fibers, using Angled Polished Connectors (APC) at all fiber interfaces. (c) Result of a bad splice in the fiber link.

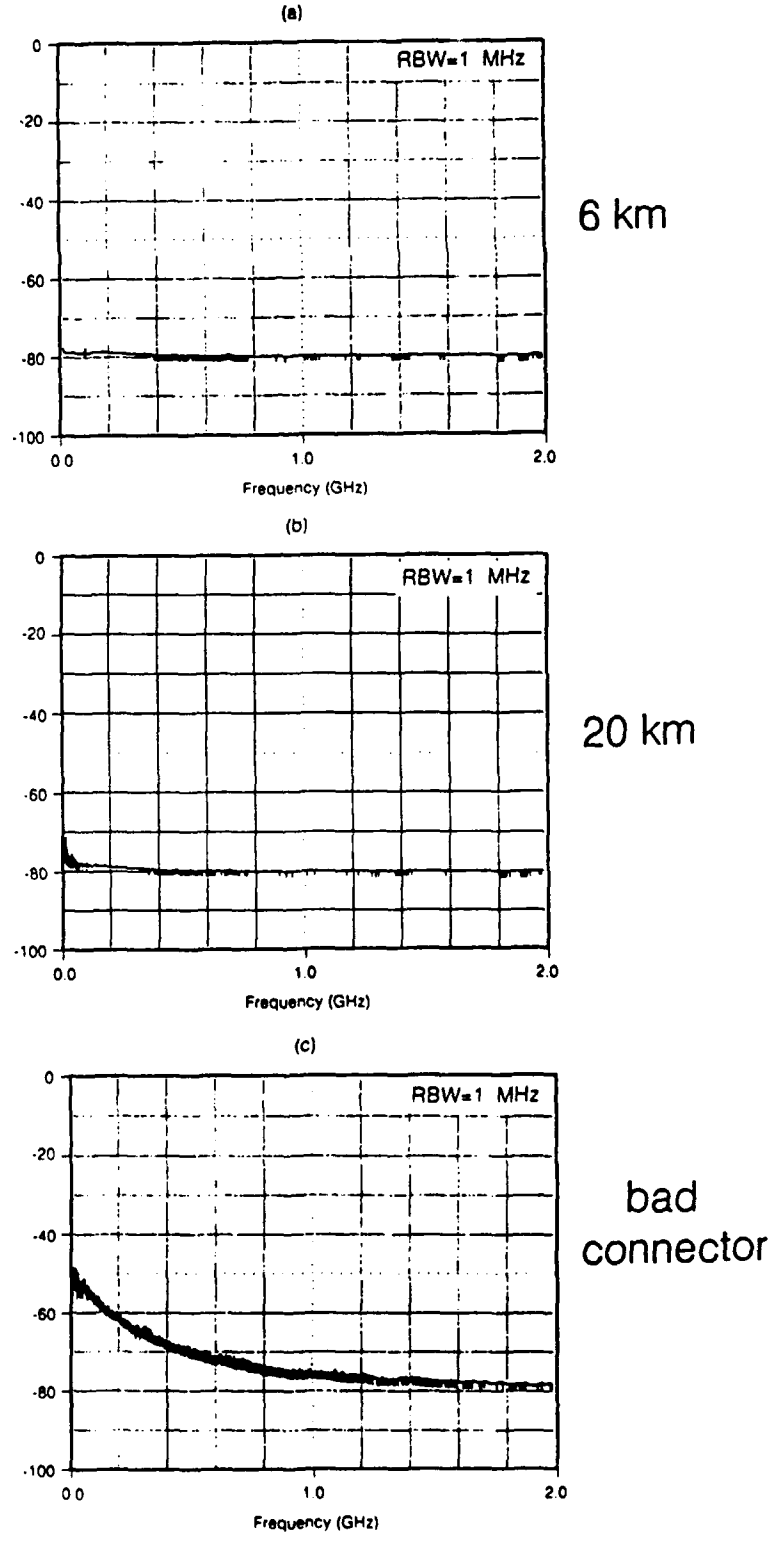

Fig. 8 Noise spectra under an applied modulation signal at +10dBm at 6.5GHz. (a)-(c): FP laser, (d)-(f): DFB laser. Three cases are show for each laser: transmission through 1km ((a) & (c)), 6km ((b) & (e)), and 20km ((c)&(f)) of single mode fibers. The DC photocurrent is adjusted to be 1mA in all the measurements except (c), which is at 0.43mA. The RF output from the photodiode is amplified by a 20dB amplifier in these measurements.

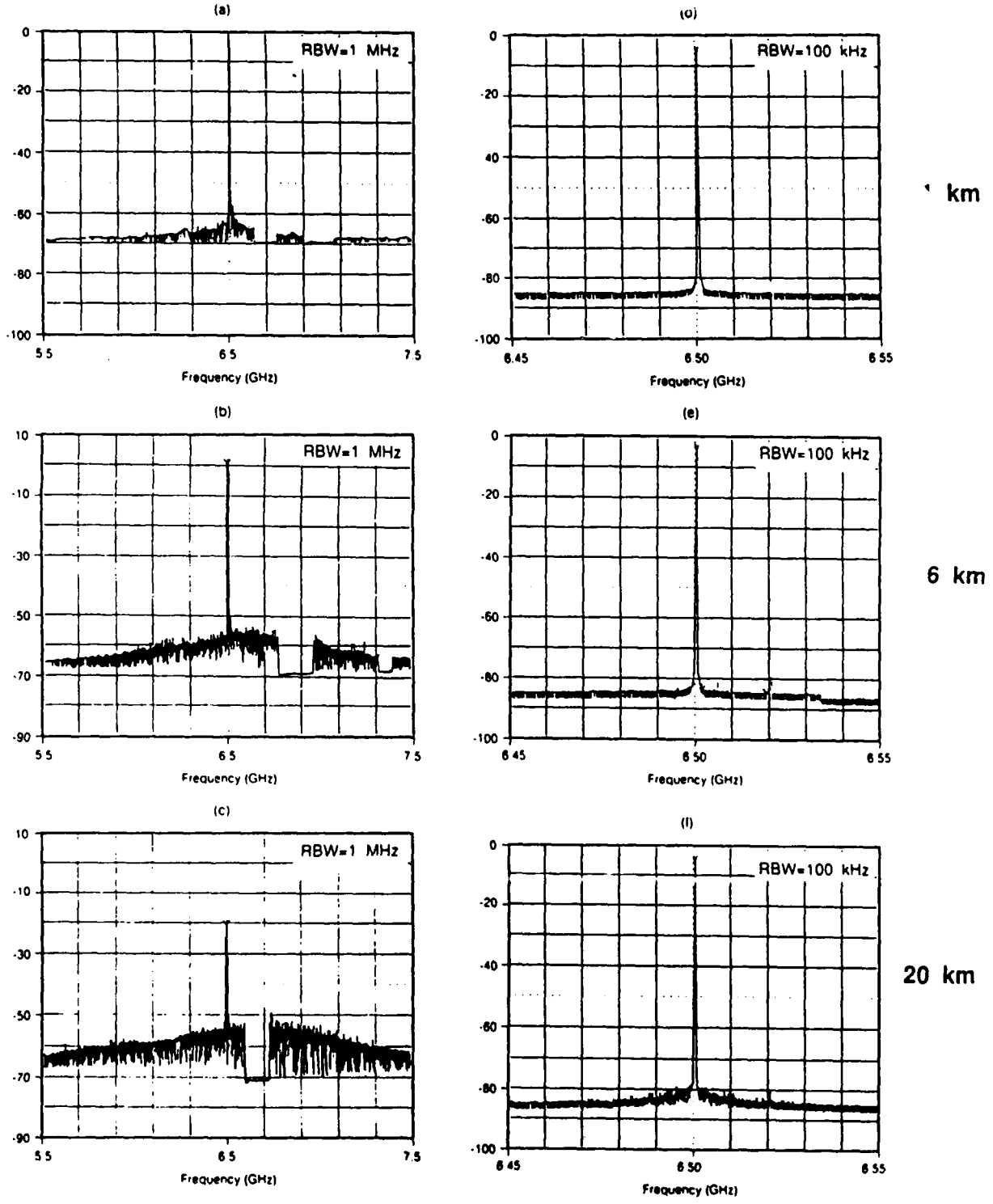

Fig. 9 Similar to Fig. 4 but at 10GHz modulation frequency.

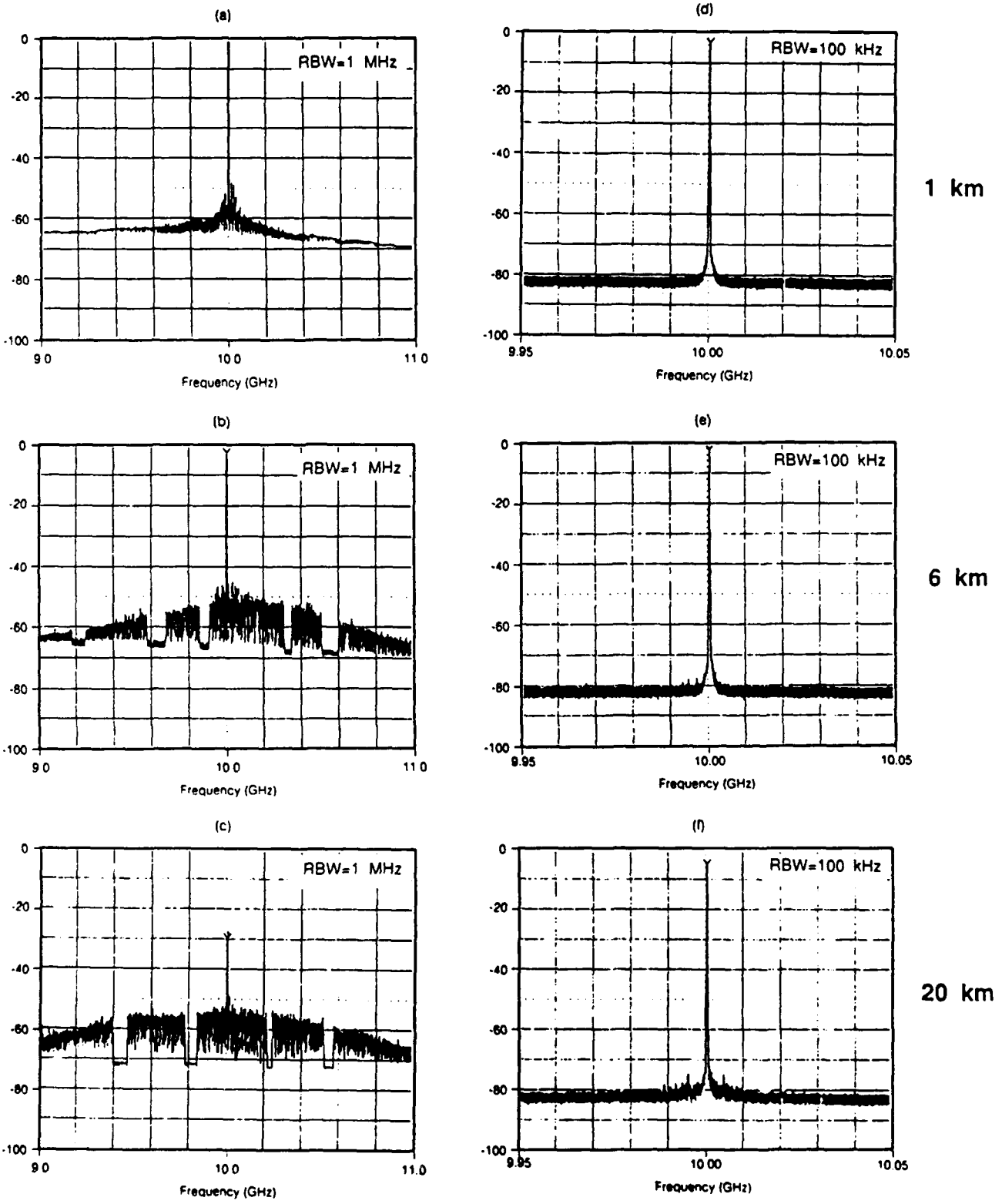

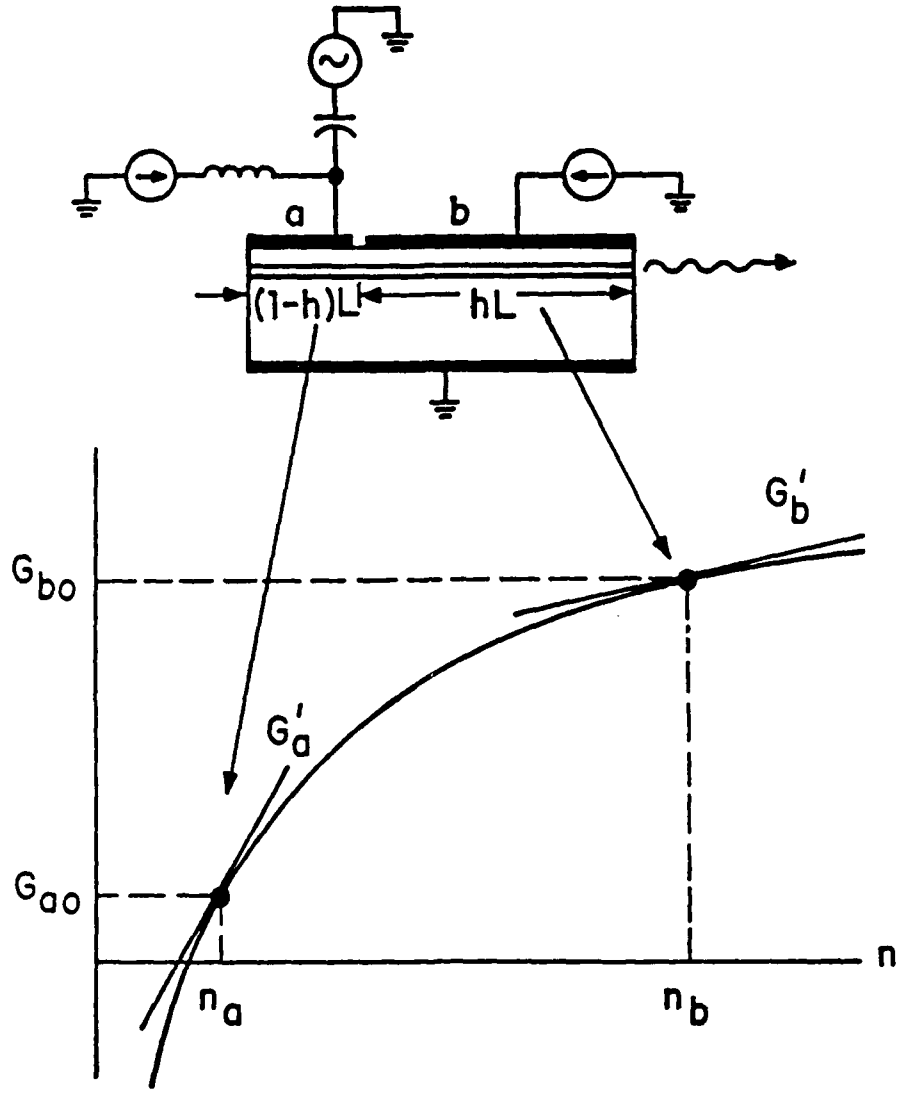

Fig. 10 Schematic diagram of a quantum well gain-levered laser.

Fig. 11 Theoretical modulation response for a split contact quantum well gain-levered laser, as compared to that of a uniformed pumped laser.

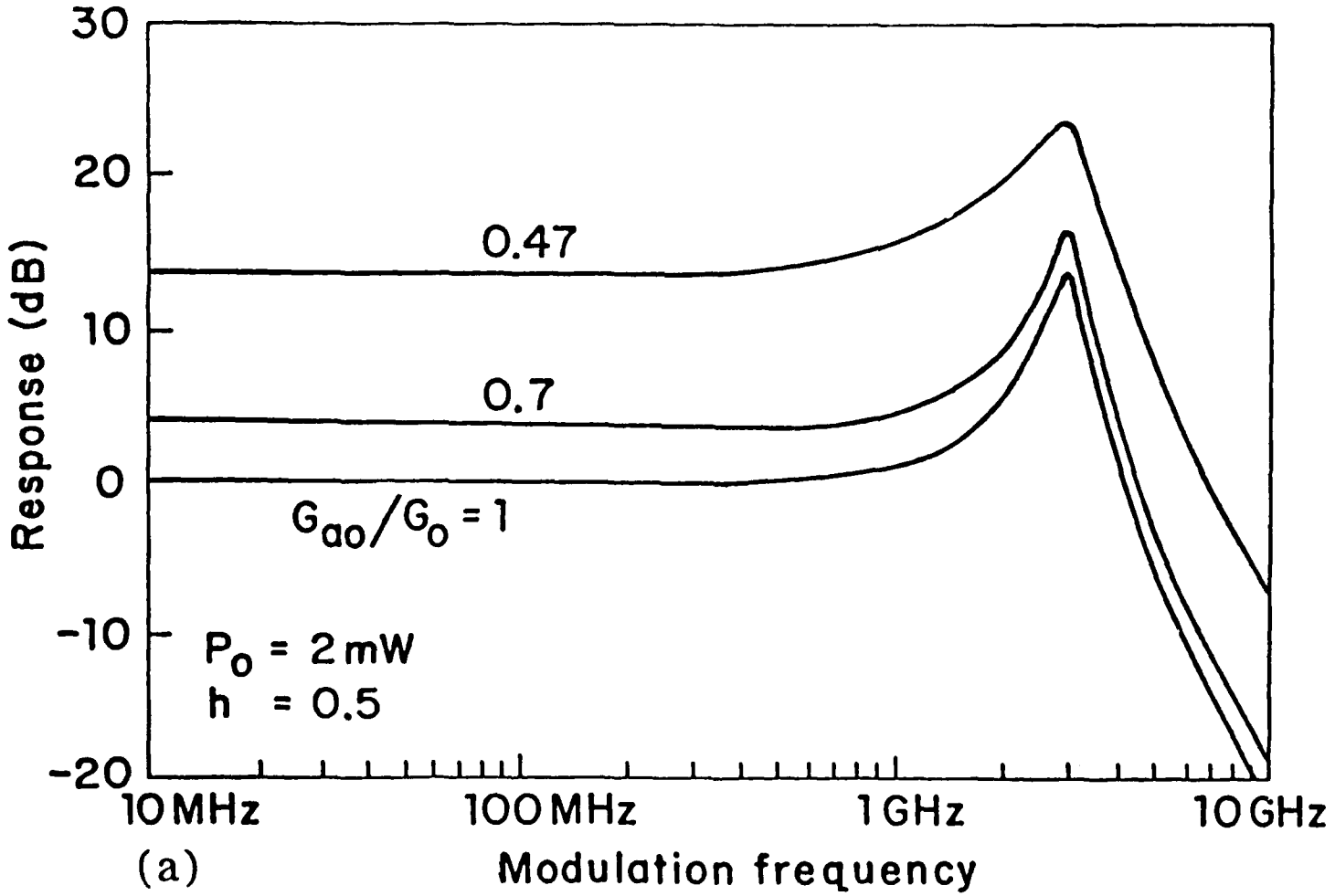

Fig. 12 Measured modulation response at output powers of 1.5mW and 4mW. Thin curves: uniformly pumped, thick curves: tandem pumped with G_{a0}/G_0=0.2 and a 220μm cavity with h=0.65.

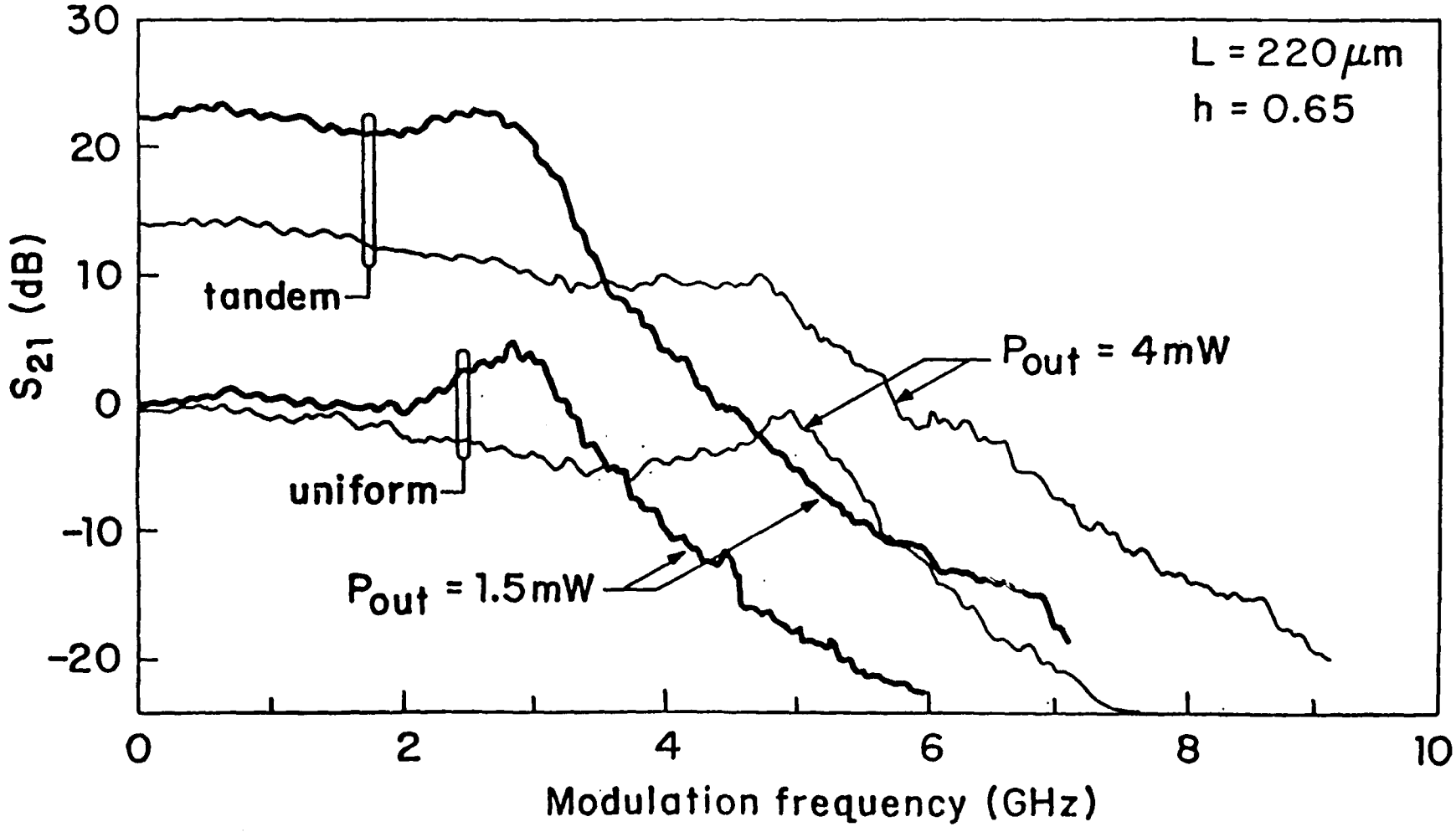

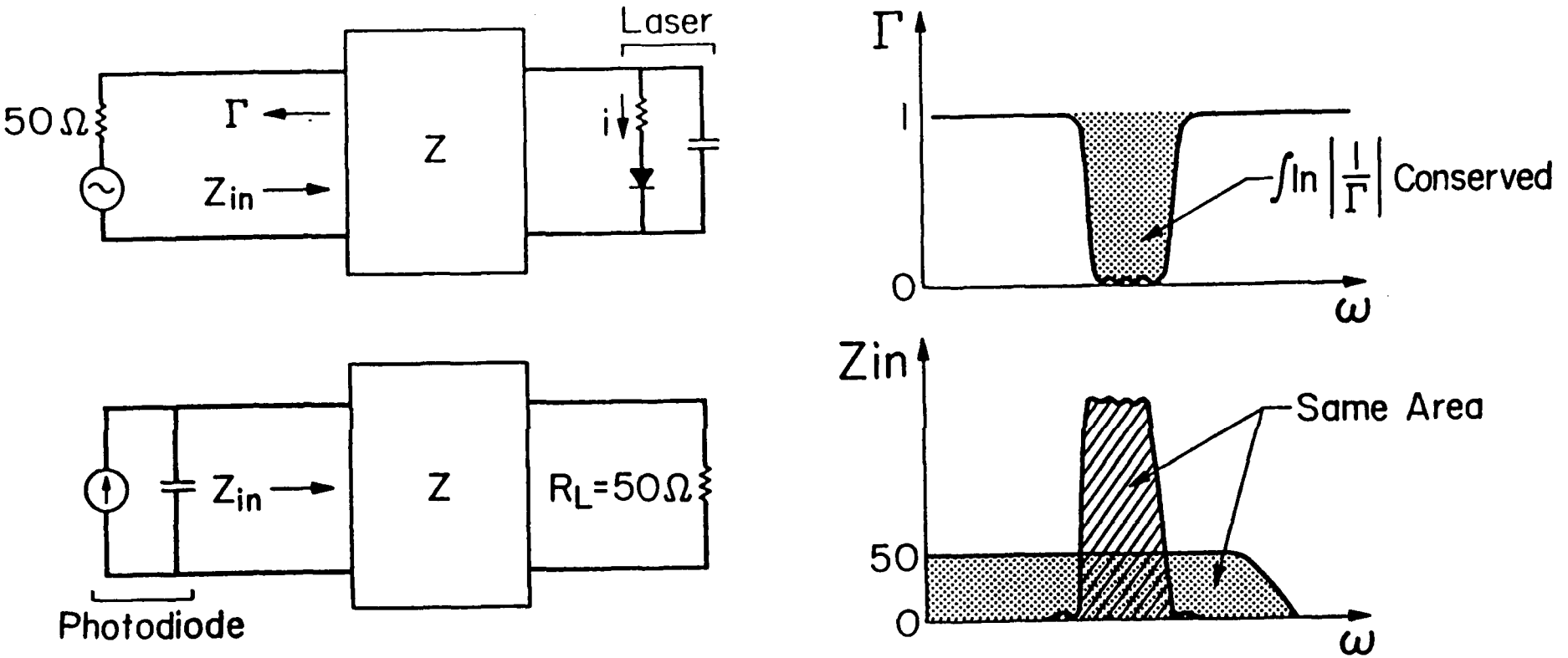

Fig. 13 (a) Schematic diagram of impedance matching of laser and photodiodes.

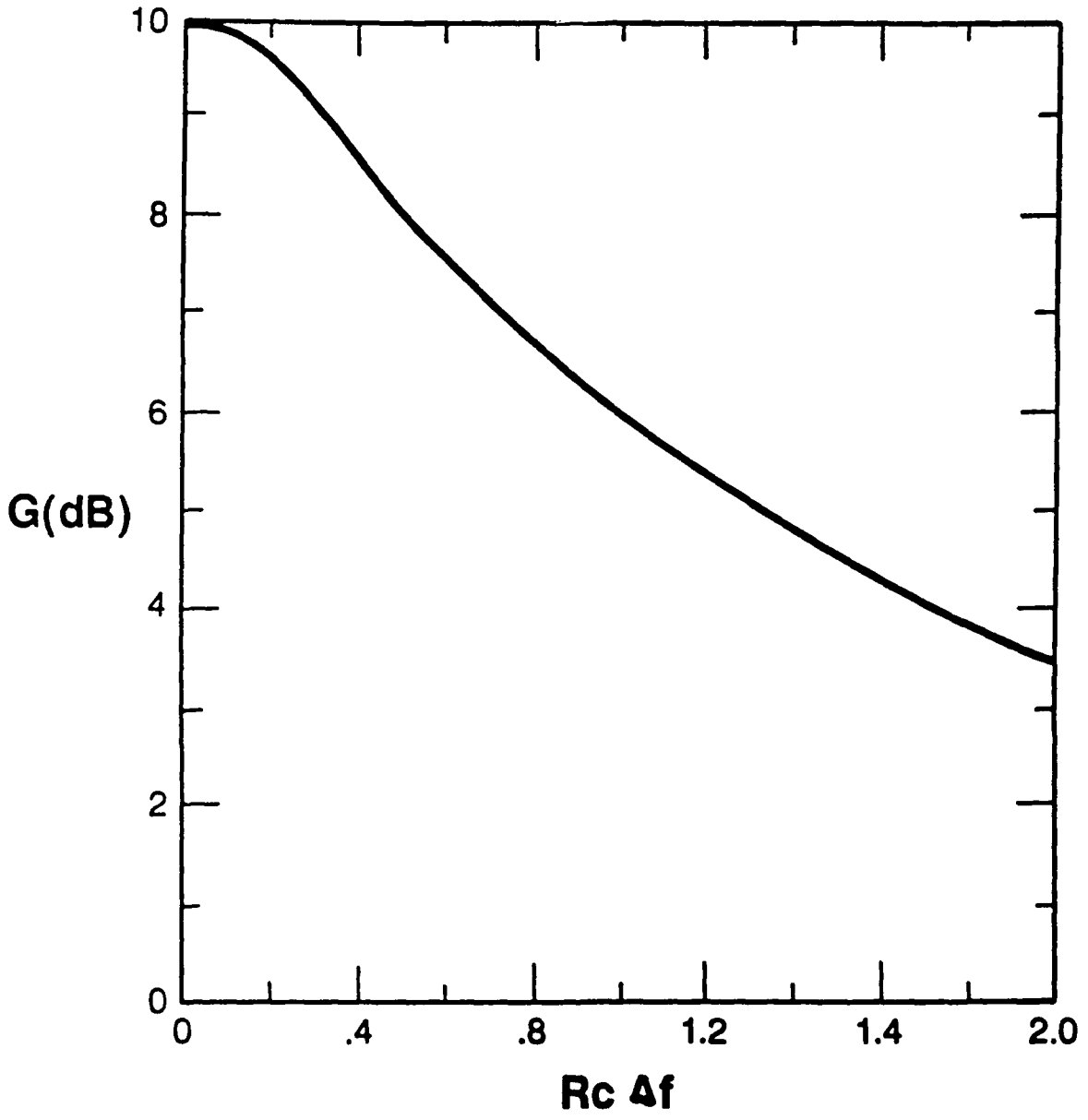

Fig. 13 (b) gain in a narrow-band matched laser diode as a function of matching bandwidth Δf normalized to the RC bandwidth of the laser.

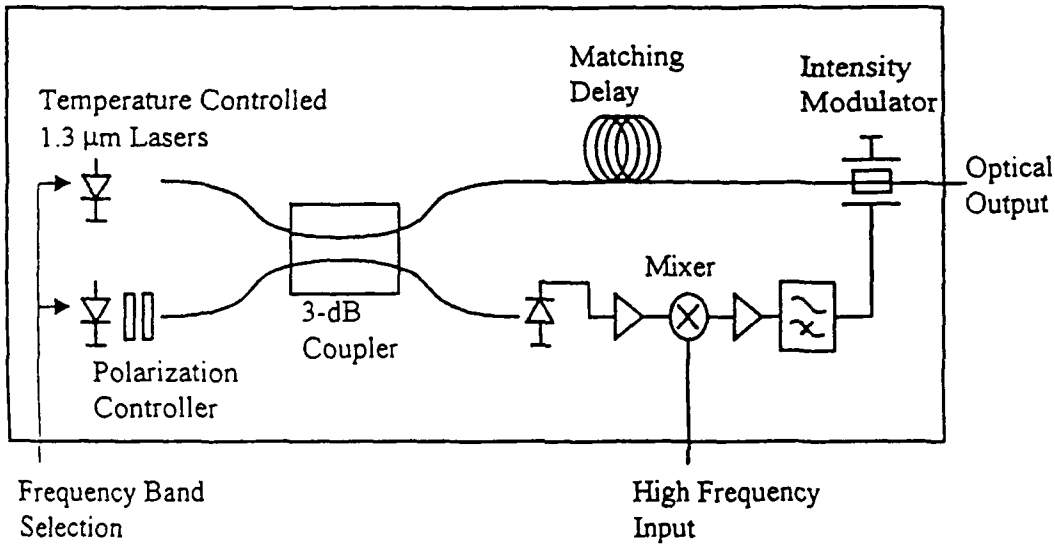

Fig. 14 **Schematic drawing shown the operational principle of the millimeter wave transmision technique.**

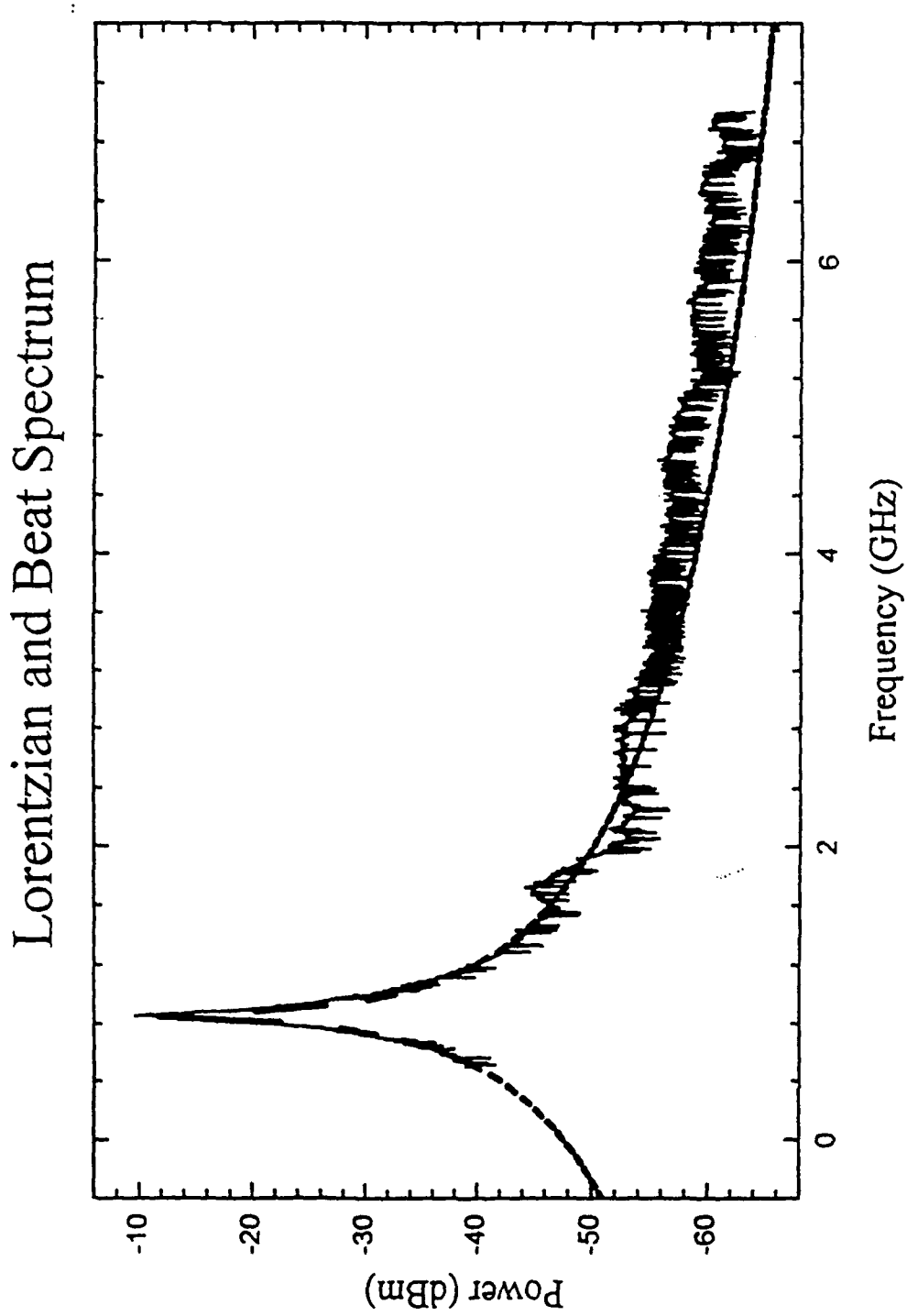

Fig. 15 Laser beatnote intensity spectrum.

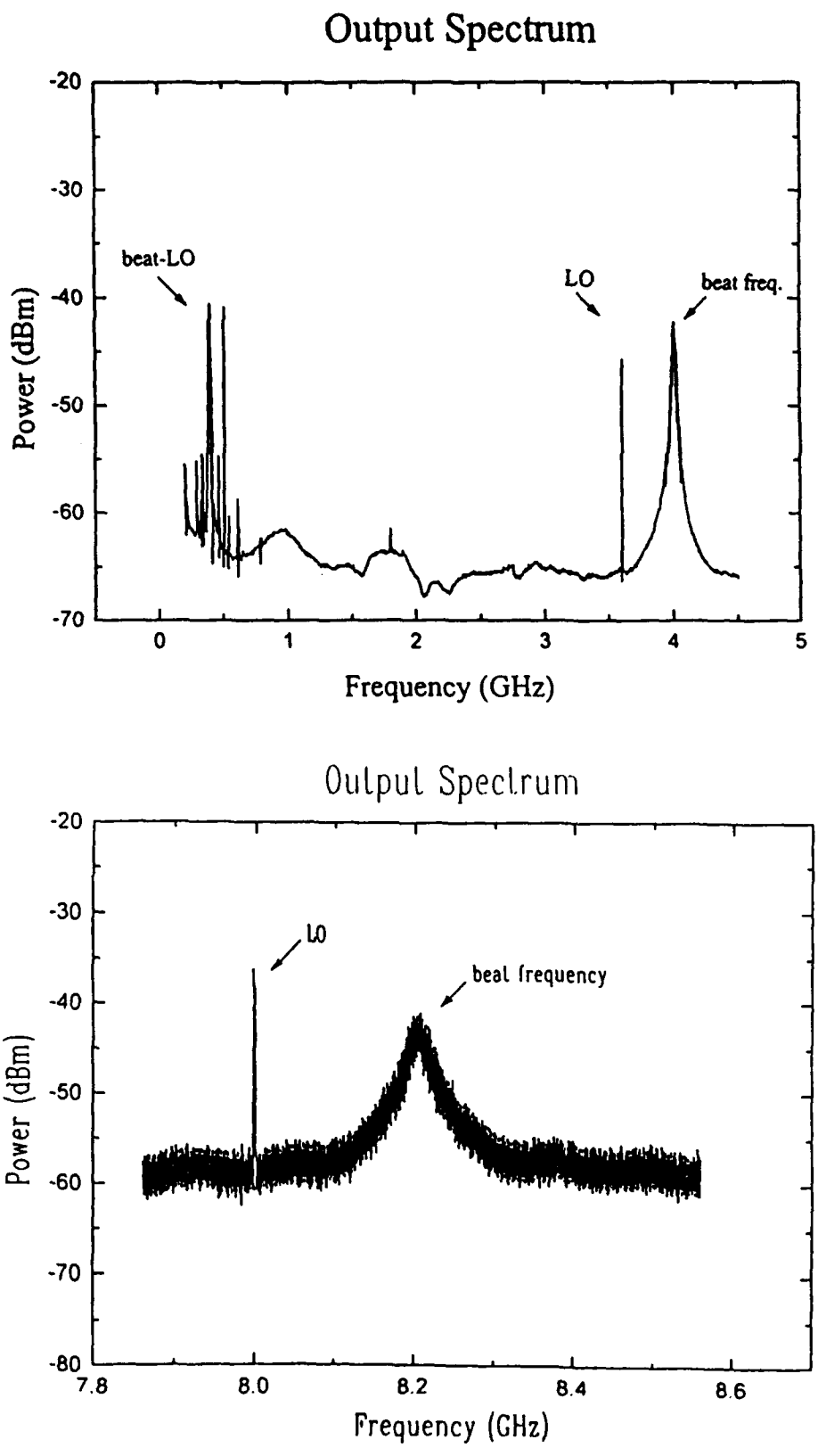

Fig. 16 **Spectrum of the optical output of feedforward transmission scheme.**

Fig. 17 S/N ratio for various relative delays of the two arms in Fig. 14.

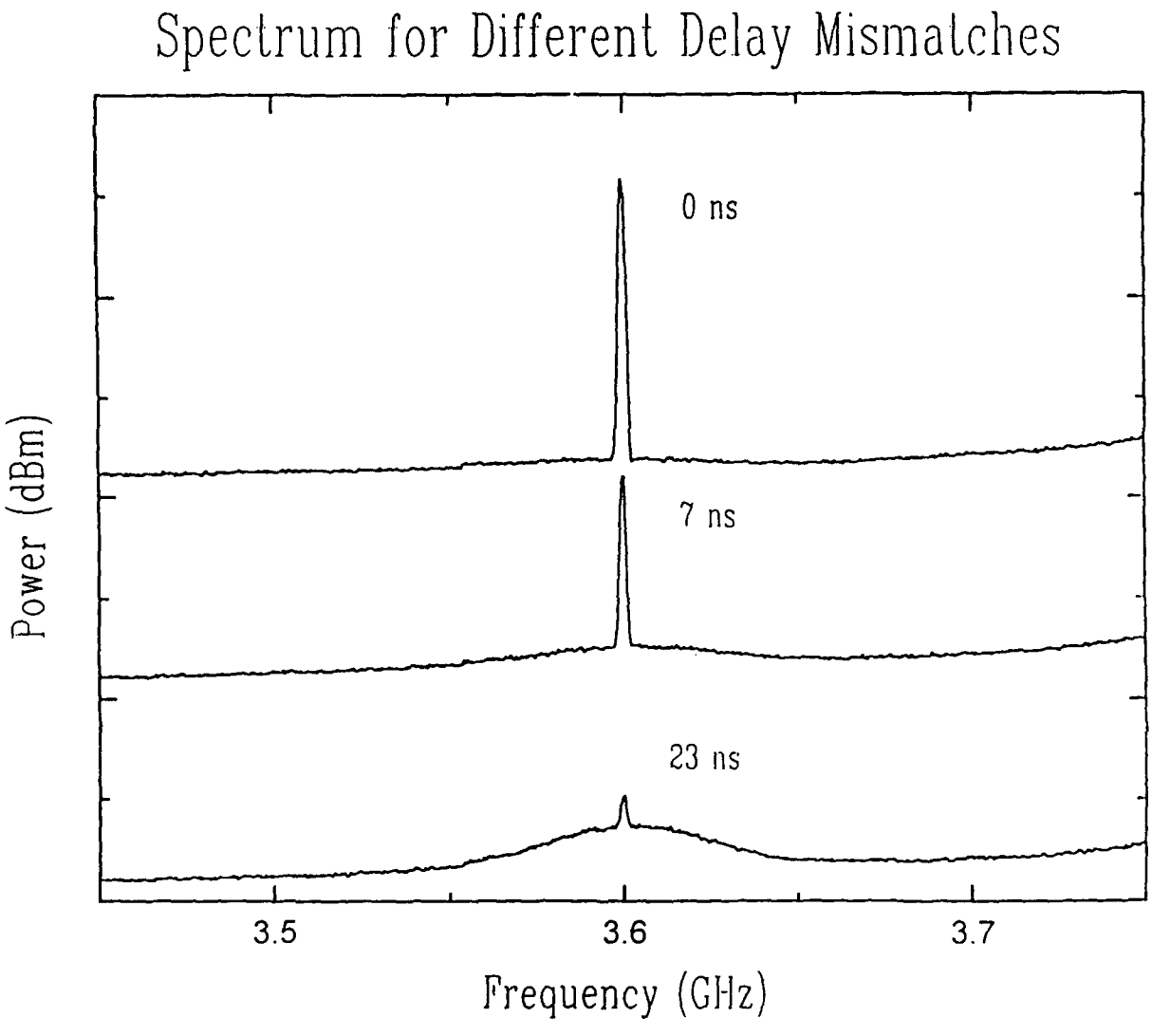

*U.S. GOVERNMENT PRINTING OFFICE: 1993-710-093-60279

MISSION

OF

ROME LABORATORY

Rome Laboratory plans and executes an interdisciplinary program in research, development, test, and technology transition in support of Air Force Command, Control, Communications and Intelligence (C^3I) activities for all Air Force platforms. It also executes selected acquisition programs in several areas of expertise. Technical and engineering support within areas of competence is provided to ESD Program Offices (POs) and other ESD elements to perform effective acquisition of C^3I systems. In addition, Rome Laboratory's technology supports other AFSC Product Divisions, the Air Force user community, and other DOD and non-DOD agencies. Rome Laboratory maintains technical competence and research programs in areas including, but not limited to, communications, command and control, battle management, intelligence information processing, computational sciences and software producibility, wide area surveillance/sensors, signal processing, solid state sciences, photonics, electromagnetic technology, superconductivity, and electronic reliability/maintainability and testability.